

**SOLAR POWER SATELLITE  
SYSTEM DEFINITION STUDY**

NASA CR-

160744

Laser SPS Analysis

Boeing Aerospace Company  
P. O. Box 3999  
Seattle, Wash. 98124

(NASA-CR-160744) SOLAR POWER SATELLITE  
SYSTEM DEFINITION STUDY. VOLUME 3: LASER  
SPS ANALYSIS, PHASE 3 Final Report, Dec.  
1979 - May 1980 (Boeing Aerospace Co.,  
Seattle, Wash.) 99 p HC A05/MF A01 CSCL 10A G3/44

N80-27811

Unclass  
28123

Contract  
NAS9-15636

June, 1980  
D180-25969-3

**FINAL REPORT FOR PHASE III, DECEMBER 1979-MAY 1980**

**VOLUME 3**

Prepared for  
LYNDON B. JOHNSON SPACE CENTER  
HOUSTON, TEXAS 77098



1. Report No.	2. Government Accession No.	3. Recipient's Catalog No.	
4. Title and Subtitle <b>SOLAR POWER SATELLITE SYSTEM DEFINITION STUDY, PHASE III, FINAL REPORT, VOL. 3 - LASER SPS ANALYSIS</b>		5. Report Date <b>June 1980</b>	6. Performing Organization Code
		8. Performing Organization Report No. <b>D180-25969-3</b>	
7. Author(s)		10. Work Unit No.	11. Contract or Grant No. <b>NAS9-16539</b>
9. Performing Organization Name and Address <b>Boeing Aerospace Company P. O. Box 3999 Seattle, Washington 98124</b>		13. Type of Report and Period Covered <b>Final Report Dec. '79 - May '80</b>	
		14. Sponsoring Agency Code	
12. Sponsoring Agency Name and Address <b>National Aeronautics and Space Administration Lyndon B. Johnson Space Center Houston, Texas 77058 (Harold Benson, Technical Monitor)</b>			
15. Supplementary Notes			
16. Abstract  This document contains the analysis of laser solar power satellite options analyzed in the Phase III Solar Power Satellite System Definition Study.			
17. Key Words (Suggested by Author(s)) <b>Solar Power Satellite (SPS) Space Power System Laser SPS</b>		18. Distribution Statement	
19. Security Classif. (of this report) <b>UNCLASSIFIED</b>	20. Security Classif. (of this page) <b>U</b>	21. No. of Pages	22. Price*

\*For sale by the National Technical Information Service, Springfield, Virginia 22161

**D180-25969-3**

## **FOREWORD**

The SPS System Definition Study was initiated in June of 1978. Phase I of this effort was completed in December of 1978 and was reported in seven volumes (Boeing document number D180-25037-1 through -7). Phase II of this study was completed in December of 1979 and was completed in five volumes (Boeing document number D180-25461-1 through -5). The Phase III of this study was initiated in January of 1980 and is concluded with this set of study results published in five volumes (Boeing document number D180-25969-1 through -5):

**Volume 1 - Executive Summary**

**Volume 2 - Final Briefing**

**Volume 3 - Laser SPS Analysis**

**Volume 4 - Solid State SPS Analysis**

**Volume 5 - Space Transportation Analysis**

These studies are a part of an overall SPS evaluation effort sponsored by the U. S. Department of Energy (DOE) and the National Aeronautics and Space Administration (NASA).

This series of contractual studies were performed by the Large Space Systems Group of the Boeing Aerospace Company (Gordon Woodcock, Study Manager). The study was managed by the Lynden B. Johnson Space Center. The Contracting Officer is David Bruce. The Contracting Officer's Representative and the study technical manager is Tony Redding.

The subcontractors on this study were the Grumman Aerospace Company (Ron McCaffrey, Study Manager) and Math Sciences Northwest (Dr. Robert Taussig, Study Manager).

# TABLE OF CONTENTS

	Page
1.0 INTRODUCTION . . . . .	1
1.1 PROBLEM STATEMENT. . . . .	1
1.2 STUDY OBJECTIVES . . . . .	2
2.0 PROPAGATION . . . . .	3
2.1 INTRODUCTION . . . . .	3
2.2 CO <sub>2</sub> LASER ATMOSPHERIC PROPAGATION CONSIDERATION . . .	3
2.3 CO LASER ATMOSPHERIC PROPAGATION CONSIDERATION. . . .	5
2.4 CO <sub>2</sub> LASER TRANSMISSION. . . . .	5
2.5 CO LASER TRANSMISSION . . . . .	5
2.6 CLOUD COVER . . . . .	7
2.7 TRANSMITTING APERTURE . . . . .	7
3.0 LASER SATELLITE OPTIONS. . . . .	10
3.1 OPTIONS SURVEY AND SELECTION . . . . .	10
3.2 ELECTRIC DISCHARGE GAS LASERS. . . . .	12
3.3 INDIRECTLY OPTICALLY PUMPED LASERS (IOPL'S) . . . . .	20
3.4 FREE ELECTRON LASERS. . . . .	30
4.0 LASER POWER RECEIVERS . . . . .	52
4.1 INTRODUCTION . . . . .	52
4.2 PHOTOVOLTAICS . . . . .	52
4.3 LASER THERMAL POWER RECEIVER. . . . .	53
4.4 OPTICAL RECTENNAS . . . . .	56
4.5 SUMMARY. . . . .	58
5.0 INDIRECT OPTICALLY PUMPED (IOP) LASER SPS CONSTRUCTION . .	60
5.1 Construction Operations Requirements. . . . .	62
5.1.1 Satellite Construction Timeline & Analysis. . . . .	64
5.1.2 Concentrator Construction Requirements . . . . .	66
5.1.3 Other Construction Requirements . . . . .	70

**TABLE OF CONTENTS**

	<b>Page</b>
<b>5.2 Laser SPS Construction Base . . . . .</b>	<b>73</b>
5.2.1 Concentrator Assembly Facility . . . . .	75
5.2.2 Final System Mating Arrangement . . . . .	75
5.2.3 Construction Equipment & Crew Operations . . . . .	77
5.2.4 Net Impact of IOP Laser SPS on GEO Base . . . . .	77
 <b>6.0 OPERATIONAL ASPECTS . . . . .</b>	 <b>83</b>
 <b>7.0 NEW TECHNOLOGY . . . . .</b>	 <b>87</b>
 <b>8.0 CONCLUSIONS . . . . .</b>	 <b>88</b>
 <b>9.0 RECOMMENDATIONS . . . . .</b>	 <b>90</b>

## ACRONYMS AND ABBREVIATIONS

### Expressions

SPS	-	Solar Power Satellite
MPTS	-	Microwave Power Transmission System
EDL	-	Electric Discharge Laser
FEL	-	Free Electron Laser
GDL	-	Gas Dynamic Laser
OPL	-	Optically Pumped Laser
IOPL	-	Indirectly Optically Pumped Laser
e-beam	-	Electron Beam
Gw	-	Gigawatt = $10^9$ w

### Materials

CO	-	Carbon Monoxide
CO <sub>2</sub>	-	Carbon Dioxide
He	-	Helium
H <sub>2</sub> O	-	Water
N <sub>2</sub>	-	Nitrogen
K Cl	-	Potassium Chloride
Zn Se	-	Zinc Selenide

## 1.0 INTRODUCTION

### 1.1 PROBLEM STATEMENT

The potential use of lasers provides an alternative to microwave power transmission offering two potential benefits. Economically, the most important is that laser power transmission may provide a means of transmitting much smaller blocks of power than is practical with microwaves. This could broaden the potential market for SPS power to include users that cannot handle thousands of megawatts of power per generating unit. The second potential advantage is that the laser option is not subject to concerns regarding the possibility of long term low level microwave energy effects on the environment.

These potential advantages are counterpoised by major issues. Perhaps foremost is the difficulty of achieving high-efficiency power transfer. State-of-the-art continuous-operation lasers such as CO<sub>2</sub> EDL's operate at efficiencies on the order of 20 to 30%, whereas the comparable microwave system is expected to operate at about 80%. Similar problems exist at the receiving end; microwave-to-DC conversion is expected to be about 80% efficient whereas laser light conversion efficiencies over 50% may be difficult to achieve. Other important issues include the laser system complexity and personnel and public safety, as well as the availability of laser power considering atmosphere propagation characteristics.

In the efficiency area, it is important to find a means of substantially improving at least one end of the link. Several means have been suggested. Some of the more significant are: (1) Use of a free-electron laser—its ideal efficiency is quite high, similar to microwave converters; (2) Direct optical pumping of the laser by sunlight (or indirect pumping through a cavity absorber within which the laser is pumped by spectrum-shifted light)—this approach eliminates the solar array and the laser efficiency may then be compared with that of the combined solar array-microwave system; (3) On the ground end, conversion by very high efficiency heat engines, by optical diodes, or by photovoltaics tailored to the laser frequency. Some combination of these options would appear to offer considerable leverage in improving the efficiency picture.

Safety and availability issues are both subject to amelioration by suitable frequency selection and avoidance of very high intensities on the ground. Thus the analysis must

consider frequency selection for safety as well as for device compatibility and efficiency factors.

## **1.2 STUDY OBJECTIVES**

This report describes an analysis of laser power transmission for SPS. This is one of 3 major tasks conducted under Phase III of the Solar Power Satellite Systems Definition Study, Contract NAS9-15636.

The objectives of the laser power transmission analysis were:

- (1) To evaluate and select laser technologies having promise for the SPS power transmission application on the basis of present and projected performance, technology risks, costs, efficiency, safety, reliability, maintainability, producibility, and power grid compatibility (propagation effects);
- (2) To develop candidate SPS system concepts using laser power transmission;
- (3) To select a "reference" system and provide a comprehensive evaluation thereof; and
- (4) To determine critical issues associated with laser SPS systems and develop a five-year ground-based exploratory development plan for key elements of the laser SPS system.



## 2.0 PROPAGATION

### 2.1 INTRODUCTION

Except for the free electron laser, which has variable wavelength, the laser types considered in this study were all CO<sub>2</sub> and CO lasers. Thus, the propagation study undertaken here emphasized finding transmission efficiencies for achievable CO<sub>2</sub> laser wavelengths near 10 microns and CO wavelengths near 5 microns. As the 10 micron CO<sub>2</sub> lines offered relatively good (.9 - .95) transmission efficiency, a global search for the best downlink laser line for the FEL to use was felt to be of little consequence and was not undertaken.

The selection of ground station sites is based upon low cloud cover and low absorption in the atmosphere. This criteria leads one to choose high altitude sites in arid climate locations, such as New Mexico, Arizona, Nevada, Utah, etc. The data presented below is characteristic of a ground station placed at a 2.3 km altitude in such an area. A lower altitude location (1.3 km altitude) will reduce the transmission characteristics for both CO<sub>2</sub> and CO lasers because of the absorption from increased water vapor in the atmosphere. A selected example is given below for both the CO and CO<sub>2</sub> laser wavelengths.

### 2.2 CO<sub>2</sub> LASER ATMOSPHERIC PROPAGATION CONSIDERATIONS

The major absorption is caused by atmospheric water vapor and atmospheric CO<sub>2</sub>. Using a carbon or oxygen isotope, one can generally eliminate the absorption problem from atmospheric C<sup>12</sup>O<sub>2</sub><sup>16</sup>, leaving water vapor as the most abundant absorber. Considering all probable isotopes and transitions, CO<sub>2</sub> lasers can operate at discrete wavelengths over the 8.9 to 11.5 micron wavelength band. Absorption from the water vapor continuum varies slowly over this band, with a trend of higher absorption at longer wavelengths. Figure 2-1 shows low resolution absorption spectra of molecular atmosphere constituents. It is apparent that judgement in selecting isotopes and the particular lasing transition must be used. Ozone has a very strong absorption band centered at 9.6 microns and a weaker band at 9 microns. Carbon dioxide (C<sup>12</sup>O<sub>2</sub><sup>16</sup>) has two bands at 9.4 and 10.4 microns. In addition, care must be taken to avoid some of the weaker absorption lines of water vapor in this region, and also, potentially very strong absorption lines from atmospheric industrial pollutants.

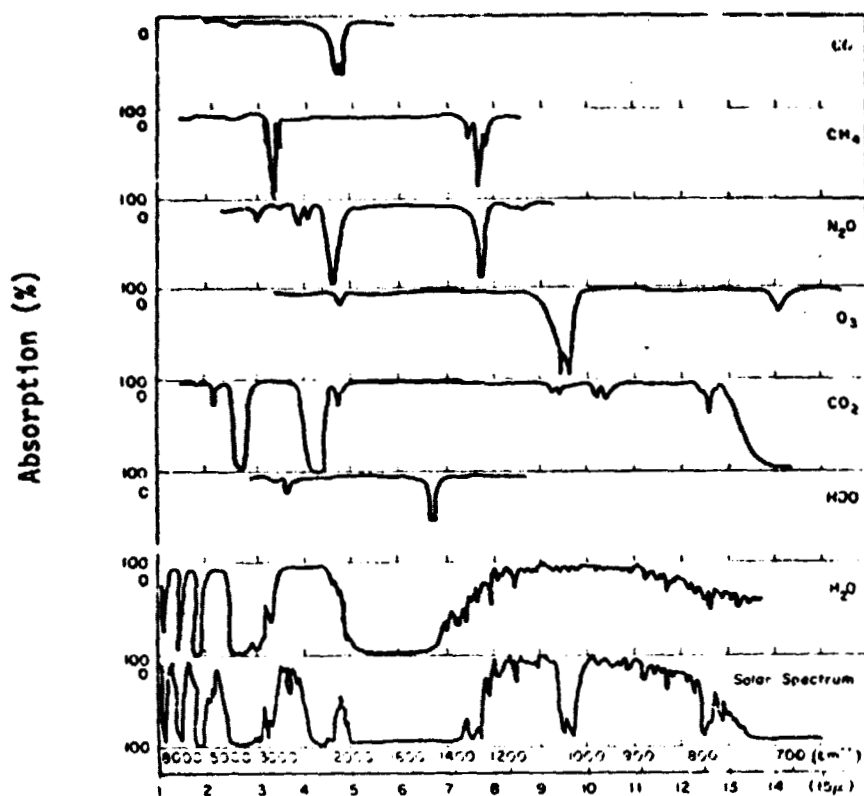


Figure 2-1: Low Resolution Spectra of Atmospheric Gases

ORIGINAL PAGE IS  
OF POOR QUALITY

### 2.3 CO LASER ATMOSPHERIC PROPAGATION CONSIDERATIONS

Atmospheric CO, in general, is not a problem, since the laser operates on the upper vibrational transitions which are not highly populated at normal temperatures encountered in the atmosphere. However, potential overlap with lower vibrational, high rotational transitions has to be considered. CO<sub>2</sub> has bands at 4.77, 4.84 and 5.7 microns which have to be avoided by choosing the CO laser transitions. Ozone, with a relatively weak band at 4.75 microns also requires attention. Of the major atmospheric molecular constituents, the strong 6.3 microns water vapor band causes most of the absorption problems associated with transmitting CO laser wavelengths thru the atmosphere. The use of CO isotopes in the laser generally does not help, since they tend to shift the laser wavelength closer to the water vapor absorption band. However, the highest atmospheric transmission can probably be achieved with line selected operation of CO or C<sup>13</sup>O<sup>16</sup>.

### 2.4 CO<sub>2</sub> LASER TRANSMISSION

On the average, the anticipated yearly, vertical atmospheric transmission value for a CO<sub>2</sub> laser is  $T = 0.56$ . The transmission at an angle  $\theta$  from the local zenith is given approximately by

$$T(\theta) = T(0^\circ)^{\sec \theta}.$$

Selecting appropriate lines of isotopic CO<sub>2</sub>, one could potentially expect to achieve  $T = 0.95$  for the yearly vertical average. Figure 2-2 shows the monthly variation of transmission. If the receiving site altitude was lowered to 1.3 km (same arid region), the anticipated yearly, vertical transmission average would be reduced to  $T = 0.90$ .

### 2.5 CO LASER TRANSMISSION

The CO transmission characteristics are more complicated to describe than those for CO<sub>2</sub>, since variations in the lasing gas temperature produce different laser efficiencies, and different spectral lines, which have different transmission characteristics. The yearly, vertical transmission average for a CO laser is anticipated to be  $T = 0.68$  for an initial gas temperature of 60°K. Figure 2-2 shows the monthly variation. Table 2-1 shows the relative variation in laser output and transmission average as a function of gas

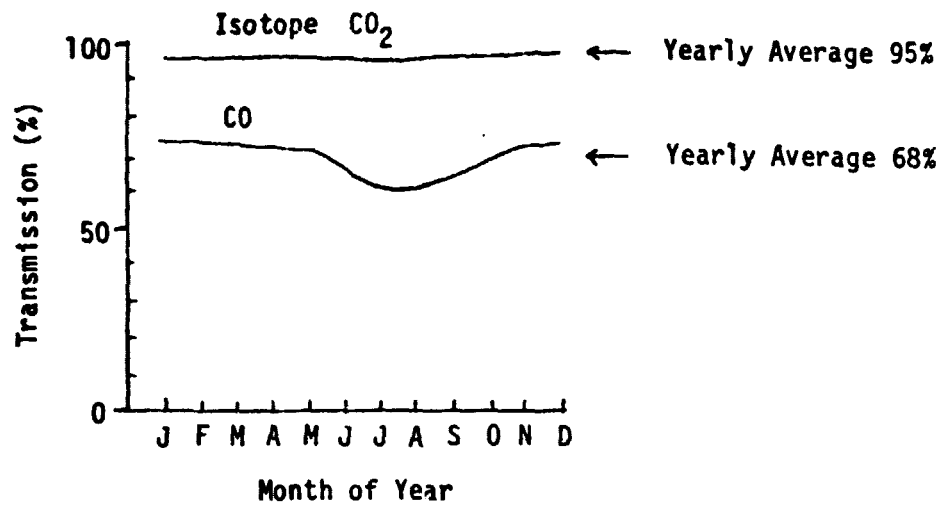


Figure 2-2: Vertical Transmission to 2.3 KM Altitude Site

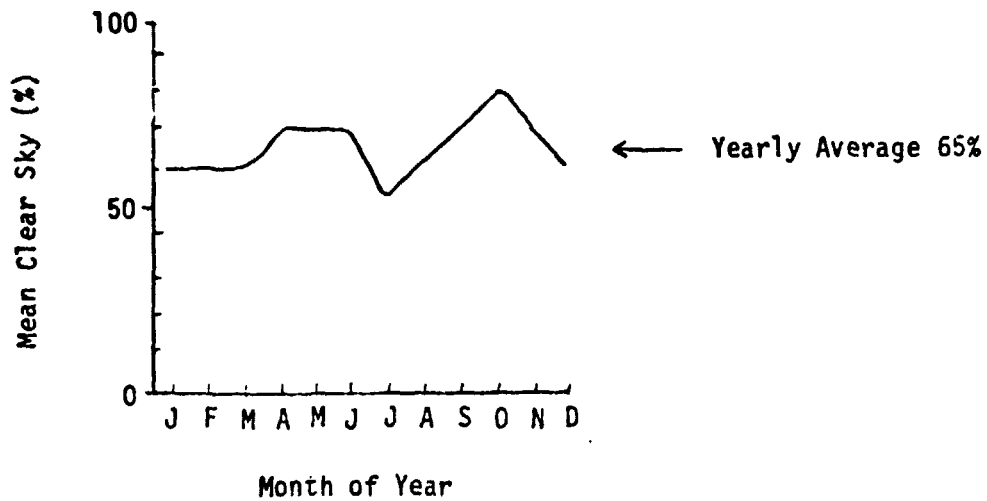


Figure 2-3: Mean Clear Sky For New Mexico Site

temperature. Reducing the receiving site altitude can have a significant effect on CO propagation. For example, lowering the site altitude to 1.3 km would reduce the nominal baseline transmission from 0.68 to 0.44. The use of an isotope gas ( $C^{13}O^{16}$ ) is projected to provide up to a 20% increase (0.68 to 0.81) in transmission, depending on estimated line selection capabilities. The relative variation with respect to temperature, altitude of receiving site, and angle off zenith, is approximately described in above examples.

## 2.6 CLOUD COVER

The dry high altitude site was selected for its high probability of cloud-free conditions as well as its low water vapor content. Figure 2-3 shows the monthly mean clear probability as well as the yearly average. Table 2-2 illustrates the yearly average overall operational probability versus the number of ground sites, assuming that each site is not located within a correlated weather system.

## 2.7 TRANSMITTING APERTURE

Based on limiting the maximum average intensity at the receiver to approximately two solar constants the optics diameter for 1 GW SPS would be 2.5 m diameter for a diffraction limited 10 micron wavelength laser. In order to account for reasonable beam quality degradation in the laser and the transmitting optics (accounting for adaptive optics correction for optics aberrations) a nominal aperture diameter of approximately 4 meters or slightly greater is considered to be of the minimum value acceptable. Mirror cooling considerations would also set this as a lower limit. Such a system could be easily controlled to provide pointing accuracies consistent with required goals. Lead angle requirements could easily be accounted for by placing the ground beacon the appropriate distance from the center of the specific ground site. Typical anticipated lead angles are in the 20 microradian regime, corresponding to a few spot diameters at the ground site. System bandwidth and gyro stability requirements would be consistent with typical round trip transit times of approximately one quarter of a second. Good isolation is required between any laser/cavity flow machinery and the optics in order to eliminate high frequency vibration coupled into the optical system. It is anticipated that careful attention to mirror cooling designs will be required to eliminate high frequency vibration of the optics due to cooling loop machinery.

D180-25969-3

Since a diffraction limited beam size is not required, it is suggested that the onboard adaptive optics control be used to produce a more nearly uniform intensity distribution at the ground receiver rather than the more sharply peaked pattern characteristic of most familiar systems. This allows more effective utilization of the received power.

**Table 2-1: CO Laser Output, Temperature, and Average Yearly Atmospheric Transmission**

<u>Laser Gas Temperature</u>	<u>Relative Laser Output</u>	<u>Yearly Average Transmission</u>
60°K	100%	68%
70°K	97%	67%
80°K	85%	56%

**Table 2-2: Availability of Ground Site Contact Versus Number of Independent Sites**

<u>Average Yearly Availability</u>	<u>Number of Stations</u>
65%	1
88%	2
96%	3
98%	4

### 3.0 LASER OPTIONS AND CONFIGURATION CONCEPTS

#### 3.1 OPTIONS SURVEY AND SELECTION

Table 3.1-1 summarizes why the following laser options were selected for analysis.

##### Electric Discharge Gas Lasers

Both the CO and CO<sub>2</sub> options are of interest. The CO system only lases well at low temperatures, i.e., below 100K, but offers higher potential efficiencies. Use of mechanical pumping systems to obtain supersonic flow in the lasing cavity may allow enough temperature recovery to permit radiation of waste heat at temperatures suitable for space radiators. Thus, there is a tradeoff among lasing efficiency, heat rejection temperature, and pumping power. A similar tradeoff exists for the CO<sub>2</sub> laser, but since the CO<sub>2</sub> laser lases well at higher temperatures, the preferred pumping power will in all likelihood be much less. The CO<sub>2</sub> laser efficiency is less than that expected for CO, so selection between these options is dependent on the tradeoff noted for each.

##### Optically Pumped Lasers

These devices are gas lasers pumped by solar energy without electric power generation as an intermediate step. Direct and indirect pumping have been proposed. The former employs sunlight concentrated directly on a lasant; the latter uses a cavity to absorb the sunlight and pumps the laser by the resulting infrared energy in the cavity. Since a lasant absorbs energy only on a relatively narrow spectral line, the direct system will be inefficient. Use of a selectively reflecting concentrator may remove the inefficiency from the laser itself and ease the thermal rejection problem. The indirect system resolves the narrow-band problem because a spectral line depleted by pumping will refill by radiative exchange with the cavity.

##### Free Electron Laser

The free electron laser (FEL) is not limited in efficiency by the Carnot limits existing for the gas lasers. The electron beam has very low entropy and the conversion to light energy



**Table 3.1-1: Laser Options First Screening**

OPTION	SELECTED BECAUSE	REJECTED BECAUSE
GLASS OR RUBY LASERS		LOW EFFICIENCY; MASSIVE
CHEMICAL LASERS		NOT SUITED FOR STEADY-STATE OPERATION
EXCIMER LASERS		LOW EFFICIENCY
SOLID STATE LASERS		LOW POWER PER DEVICE; LOW VOLTAGE; COMPLEXITY
GAS DYNAMIC LASERS		LOW EFFICIENCY AND MASSIVE
GAS ELECTRIC DISCHARGE LASERS	POTENTIAL FOR HIGH POWER AND FAIR EFFICIENCY	
GAS OPTICALLY PUMPED LASERS	ELIMINATION OF SOLAR ARRAY	
FREE-ELECTRON LASER	POTENTIAL FOR HIGH POWER AND GOOD EFFICIENCY	

in principle could be very high. There are, of course, practical problems that may limit efficiency. Present ability to predict eventual efficiency must be regarded as dubious. The FEL was included in this study because of its efficiency potential; the study estimated the FEL efficiency needed to make this option competitive with the other laser options.

### **Options Rejected**

At this point a number of laser options have been rejected as unattractive. These include gas dynamic, metal vapor and dye lasers because of their relatively low efficiencies. Chemical lasers were eliminated because of the system complexity and power losses involved in reforming lasing chemicals after lasing. Finally, the low pumping efficiencies of directly solar pumped lasers require such large solar collectors as to make them undesirable for most SPS system purposes. Thus, this subtype of optically pumped laser should also be considered an option to be rejected.

## **3.2 ELECTRIC DISCHARGE GAS LASERS**

These systems consist of a solar array that provides electric power, an electric discharge gas laser system, a thermal radiator to reject waste heat, and a set of optics to form the laser beam and direct it to the Earth receiver station (see Figure 3.2-1).

For purposes of this study, it was decided to employ electric power from the solar array to drive the compressors and pumps. The use of a solar-thermal cycle is somewhat complex unless an optical rotary joint is used (see below); for the electrical rotary joint alternative, the thermal cycle must be located on the solar array to continuously face the sun. It therefore must generate electricity as a power transfer medium. Prior SPS studies have not shown significant advantages to solar-thermal electric generation. Although that trade may merit revisiting, it was elected not to do so here. Use of electric compressor and pump drive removes a constraint from the optical/electrical rotary joint trade. (If an optical rotary joint is used, the laser systems may be located on the solar array and a solar-thermal cycle can transfer shaft power to the pumping system.)

Optical and electrical rotary joint options were compared. The optical rotary joint is constrained to two lasers per SPS (one each end), although "laser" here can be taken as a gang of phase-locked lasers forming a single beam through a single set of optics. The

ORIGINAL PAGE IS  
OF POOR QUALITY

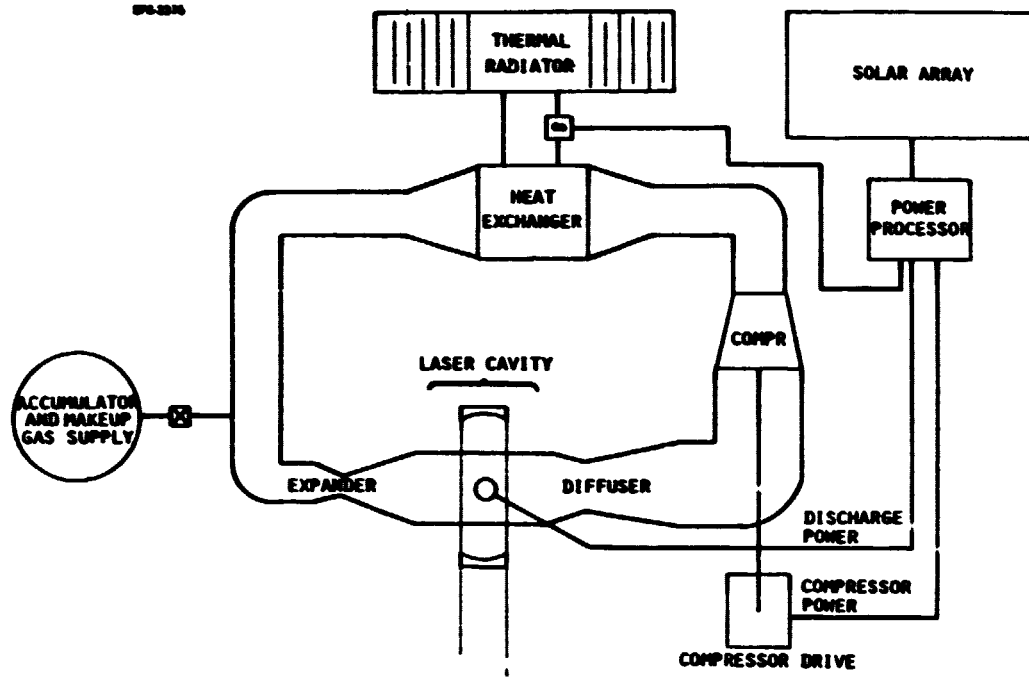


Figure 3.2-1: Electric Discharge Laser Schematic

turning flat must be controlled to provide exactly half the elevation drive provided by the beam-forming optics. Assuming the satellite is flown perpendicular to the orbit plane, the elevation drive excursions will be small. With an electrical rotary joint, the entire laser assembly is Earth-oriented and there is no constraint on the number of laser units per SPS. This option allows one SPS to generate many laser beams and serve as many ground stations as desired. Fine steering for each laser unit to keep all beams precisely on their ground stations can be provided by beam-forming optics. Selection of a configuration option depends on scaling of the electric discharge gas lasers. If these systems can be large, there is less advantage to the electric rotary joint. However, due consideration must be given to the number of assignable slots in geosynchronous orbit for SPS. Conservation of the GEO space resource is likely to require relatively large SPS's. Multiple-beam laser satellites can retain the desirable laser feature of small blocks of power per beam while providing high power rating per GEO slot.

Electrical lasers using an electron beam for sustaining a uniform discharge at high cavity pressure have a scaling limit imposed by the magnetic field of the sustainer current. This deflects the high energy electrons of the e-beam, causing non-uniform heating leading to laser medium distortions due to a non-uniform index of refraction. These distortions limit the volume or cavity size and consequently the power level that can be obtained from a single laser. Thus, the high power levels required for the SPS leads to the ganging of many laser cavities in an annular device.

Since CW operation of high pressure electrical lasers leads to mode/media interaction problems resulting in fluctuating and reduced power output, only pulsed lasers are considered for the SPS application. The pulse repetition rates considered are around 100 Hz for a subsonic laser and 1 Hz for a supersonic laser.

A typical arrangement of ganging laser modules in a cylindrical configuration is shown in Figure 3.2-2. The laser gas flow is radially outward. The cavities are sandwiched between electron guns which provide the high energy (approximately 200 keV). Each gun provides electrons to adjacent cavities. The cavities contain a center electrode which allows doubling of the cavity height while still satisfying beam quality requirements.

Although a common fluid supply system could be envisioned, use of a separate closed cycle gas flow system for each laser cavity module appears more attractive from assembly, maintenance and reliability point of view. Either subsonic or supersonic closed cycle systems would satisfy the concept shown in Figure 3.2-2.

ORIGINAL PAGE IS  
OF POOR QUALITY

D180-25969-3

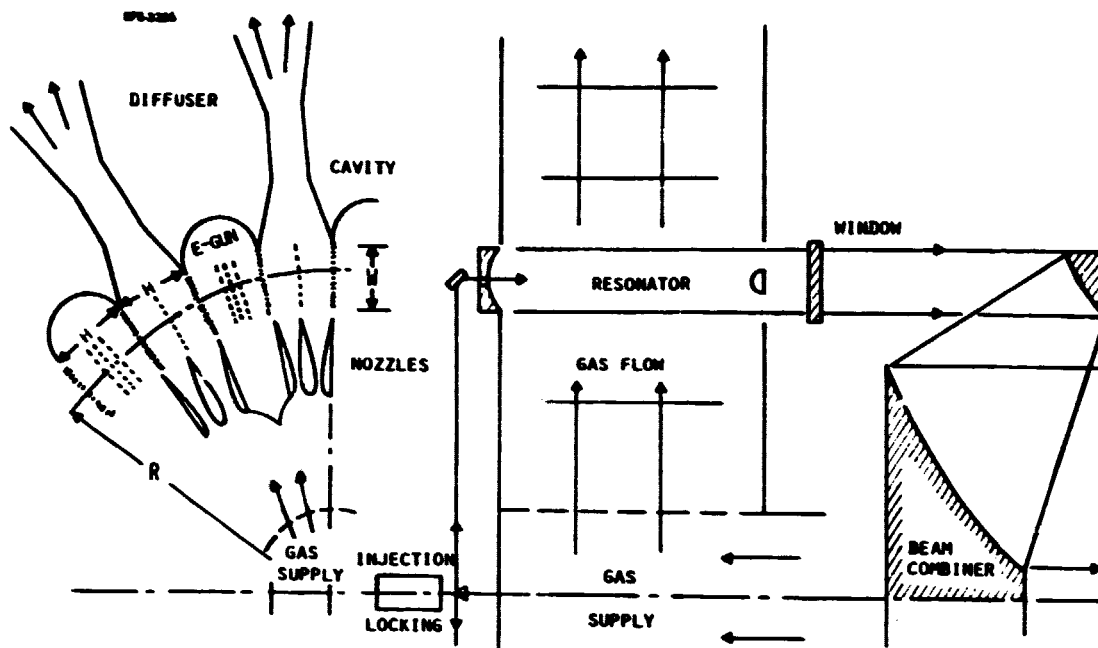


Figure 3.2-2: Electrical Discharge Laser Configuration for SPS

The individual optical resonators are phase locked using a common injection laser. The beam combining concept may utilize waxicons similar to those used in cylindrical chemical lasers.

Conventional electric discharge laser performance characteristics for supersonic flow CO, and supersonic flow and subsonic flow CO<sub>2</sub> lasers were developed for conditions relevant to an SPS application. The devices were sized for an output consistent with SPS requirements. Specific performance trades were directed toward reducing the heat rejection requirements at low temperature because of the  $T^4$  law characteristics and resultant very large area radiators (and therefore very large mass) required at low temperature. This greatly compromised laser efficiency but was unavoidable from a satellite mass and cost minimization standpoint.

A cycle trade was done to select the optimal laser Mach number. This trade considers increases in pumping power to increase the heat rejection temperature relative to the lasing cavity temperature. It is apparent that there are three primary design parameters: (1) Lasing cavity temperature and associated laser efficiency; (2) Heat rejection temperature and associated radiator size and mass (the radiator size is also affected by system efficiency, thus depends also on laser efficiency); (3) Compressor power resulting from the selected temperatures and the gas flow rate. The compressor power also results in enthalpy added to the gas and contributes to the waste heat load. This bears on the configuration trade in terms of additional radiator requirements.

Table 3.2-1 shows some of the more important characteristics associated with specific types of laser. The subsonic CO laser was not considered since heat rejection via radiative means is unrealistic at radiator temperatures below 100°K. Thus laser cavity operation at 60°K-80°K is only feasible for a supersonic system. Closed cycle operation for a supersonic laser reduces its overall efficiency, because of the relatively large compressor power requirements. Table 3.2-1 also shows the dependence of compressor power requirements as a function of Mach number and initial cavity static temperature. In ground based systems a heat exchanger between laser exhaust and compressor is used to increase compressor efficiency. However, because of the relatively low total temperatures ( $T_p$ ) involved, this approach does not appear attractive for a space based laser without the use of a heat pump. CO<sub>2</sub> was not considered for operation at supersonic Mach numbers below  $M = 3$  because of potential problems associated with the large amount of heat release which would result in choking the flow in or immediately adjacent to the

Table 3.2-1 Electric Discharge Laser Performance Characteristics For 1 Gw Laser Output

Mach No.	Static Temp.	Total Temp.	Cooling From	Power To Cool	Total Elec. Input	Percent Comp. Power	Total Eff.	Gas Flow	Empty Wt.	Yearly Transmission (Average)
Supersonic CO Laser										
2	80°K	176°K	327°K	2.27	3.27	23%	.305	17,331 Kg/sec	1351x10 <sup>3</sup> Kg	56%
2.5	80	230	466	2.67	3.67	39	.272	15,456	956x10 <sup>3</sup>	56
3	80	296	630	3.50	4.50	52	.222	14,993	754x10 <sup>3</sup>	56
3.5	80	374	899	5.67	6.67	66	.152	13,158	655x10 <sup>3</sup>	56
2.5	60	172	360	1.87	2.87	33	.349	13,158	937x10 <sup>3</sup>	68
3	60	222	498	2.50	3.50	47	.286	12,821	720x10 <sup>3</sup>	68
3.5	60	280	609	4.38	5.38	64	.186	13,258	655x10 <sup>3</sup>	68
Supersonic CO <sub>2</sub>										
3	200	533	655-400 +635-533	2.90 +4.50 7.40	8.40	54	.119	23,256	2,300x10 <sup>3</sup>	95
Subsonic CO <sub>2</sub>										
.15	300	300	456	3.70	4.70	3.5	.212	20,408	3,100x10 <sup>3</sup>	95

Note:

1. Heat transfer equipment between heat exchanger in laser and radiator not included.
2. Weight is a rough estimate and requires conceptual designs to verify, especially for subsonic CO<sub>2</sub>.

D180-25969-3

laser cavity. This is in sharp contrast to the supersonic CO laser, where, because of the relatively long vibrational energy deactivation time, the supersonic flow can be diffused to subsonic flow conditions before the remaining discharge energy in the vibrational states can relax and produce a significant temperature rise in the laser gas.

The component masses shown in Table 3.2-1 are preliminary and are based on values predicted for previous airborne laser programs. Initial laser efficiency estimates, defined as laser energy output divided by electrical energy into the laser cavity, are 30% for CO<sub>2</sub> at 200°K, 25% for CO<sub>2</sub> at 300°K, 60% for CO at 60°K, and 51% for CO at 80°K. The Table 3.2-1 results as a function of laser cavity Mach number are charted on Figure 3.2-3 as mass for a 1 Gw delivered grid power SPS. Because of its higher radiator temperature the subsonic CO<sub>2</sub> is the least massive option even though its laser efficiency is low.

A major technology issue is associated with window cooling. The mirror cooling requirements appear to fit within present state-of-the-art technologies. The requirement to cool large diameter windows transmitting high power levels will probably necessitate the use of a film cooling component with a thermopane type design. Heat transfer rates of the order of 0.2 W/cm<sup>2</sup>-°K can probably be achieved with Mach 0.5 flow helium gas at 1 amagat density. The thermal conductivity of KCl (a material having the lowest absorption at 10.6 micron wavelength) is 0.05 W/cm-°K. This can be a very severe limit in attempting to cool high average intensities over extended periods of time. The problem is greatly aggravated because KCl will fracture from thermal shock or relatively small temperature gradients in the material. In addition, any nonuniformities in laser intensity across the aperture can increase the attendant problems. Another possible approach may be to use ZnSe for the CO<sub>2</sub> laser. Although the bulk absorption is about 2 times higher, a thermal conductivity of 0.17 W/cm-°K and a higher fracture limit and lower thermal expansion coefficient may offset the higher bulk absorption.

In addition to bulk absorption, windows also have a surface absorption which can be larger than the bulk values. Manufacture in space has the potential capability to reduce impurity levels, and thus possibly reduce surface absorption levels. Another approach would be to use a semiconductor material and cool it to less than 150°K, which could reduce free carrier absorption. Based on present technology limitations, a material window for subsonic lasers would be more feasible, because the average incident intensities are about a factor of 20 less than experienced with supersonic flow devices.



ORIGINAL PAGE IS  
OF POOR QUALITY

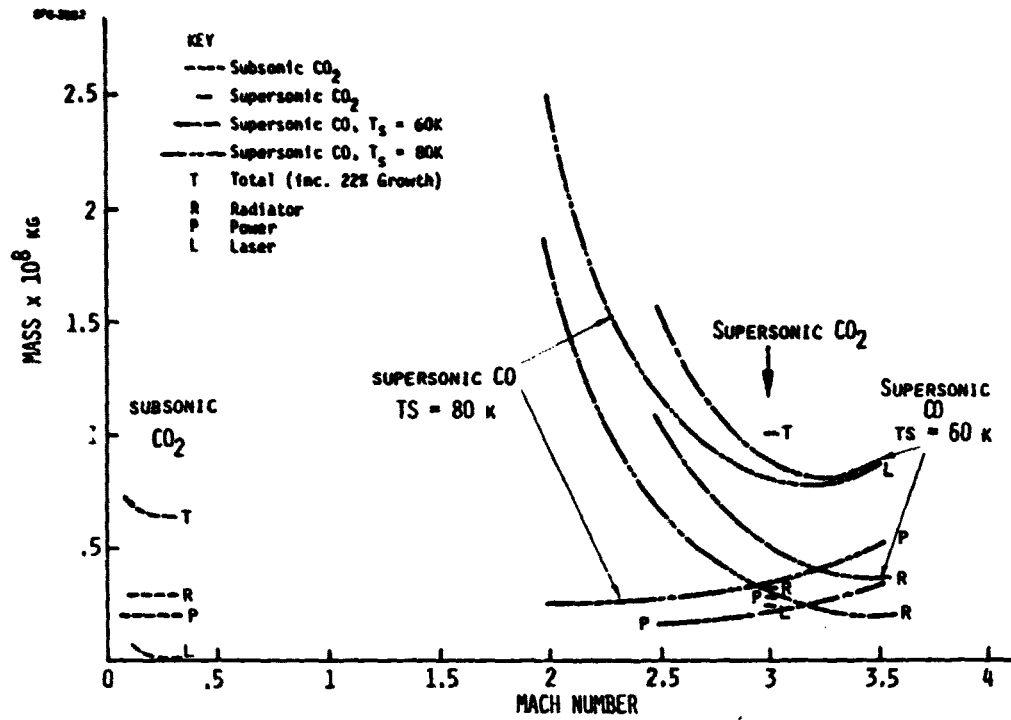


Figure 3.2-3: 1 GW EDL Laser SPS Masses vs Mach Number

Strontium fluoride appears to be one of the best window materials for the CO laser because of its relatively low bulk absorption ( $2.3 \times 10^{-4} \text{ cm}^{-1}$ ) and high fracture strength. However, a thermal conductivity of 0.074 would appear to limit the overall power handling capability. Other appropriate materials to consider include calcium fluoride and potassium chloride.

Preliminary estimates have been made for the dissociation rates for both the  $\text{CO}_2$  and CO lasers operating under anticipated electric field conditions. Dissociation of CO or  $\text{CO}_2$  by either the main discharge or the electron gun does not appear to be a major problem, mainly because the gas spends at most .002% of its time in the discharge as compared to traversing the closed cycle circuit. If it were not for this fact, the dissociation of  $\text{CO}_2$  into  $\text{O} + \text{CO}$  would pose a serious problem since its dissociation probability is about  $10^8$  times as large as the CO dissociation probability, and rough order of magnitude estimates indicate that the  $\text{CO}_2$  lifetime in a discharge would be less than a year.

### 3.3 INDIRECTLY OPTICALLY PUMPED LASERS (IOPLS)

#### 3.3.1 Introduction

The use of optical pumping of lasers is a possible way to bypass the generally low (circa .25) conversion efficiencies of sunlight into electrical power that all the other electromagnetic power transmission methods for SPS must encounter. However, the direct solar spectrum is a poor match to desirable laser pumping lines. With what may be the best lasant chosen for a direct solar pumped laser known today,  $\text{CF}_3\text{I}$  lasing at 1.315 microns, the fraction of the solar spectrum absorbed is about 2.5%. Even though the low mass per unit area of solar reflecting mirrors allows an interception of sunlight greater than for indirect conversion of solar-to-laser power schemes the order of improvement in mass per unit area is less than 10 while the value required to be more attractive than the best other options is around 20.

A much better spectral match may be provided by going to an indirect solar pumping system which concentrates sunlight on a black body cavity which reradiates a more appropriate spectrum (Figure 3.3.1). In fact, analyses of systems like this indicate that solar-to-laser light efficiencies of up to 30% may be achievable.

SP-3228

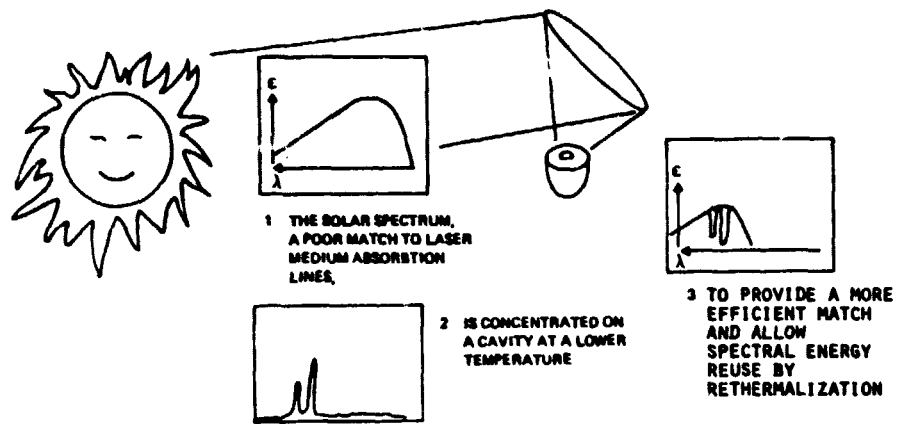


Figure 3.3-1: Indirect Optically Pumped Laser Principles

ORIGINAL PAGE IS  
OF POOR QUALITY

In this study, three such indirectly pumped laser cycles were considered in a joint effort with Mathematical Sciences Northwest, subcontractors to Boeing for this task. These three systems were conventional subsonic CO<sub>2</sub> and supersonic CO Brayton cycle lasers and a rather unique "mixing gas laser". The latter used CO as an absorbing gas for the thermal pumping spectrum and transferred the excitation energy to CO<sub>2</sub> laserant via mixing. The latter system was chosen for most detailed analysis because it was felt that there was substantial improvement potential over the other two IOPL types. It was thus also baselined for a detailed construction analysis because it represented the laser SPS option most different from the relatively well understood standard photovoltaic microwave reference SPS's.

### 3.3.2 Configuration Analysis

The most basic configuration trade is selection of the rotary joint. Both options are optical as illustrated in Figure 3.3-2. The trade considerations are similar to those for the electric gas laser. Use of a concentrator optics rotary joint allows as many lasers as desired per SPS. The laser optics rotary joint allows only two. The concentrator is somewhat more complex in the former case, being an approximation of an off-axis paraboloid. Since the concentrator need not be of image-forming quality, this does not appear to be a serious penalty. The IOPL must be flown perpendicular to the ecliptic plane (or have steerable facets an undesirable complexity) in order to maintain concentrator performance. This requires the laser optics to have +/-23.5 degrees elevation tracking capability, and in the laser rotary joint case, also 360 degrees tracking capability on the other axis.

Since this laser system option was selected for space construction analysis, a decision on the configuration size and arrangement was necessary prior to completing the scaling and cycle analyses. In order to ensure that the system not be constrained to low power levels, the concentrator rotary joint was selected. The system was sized somewhat arbitrarily to put 1 gigawatt of optical power into the cavity. This yields somewhat less than 100 megawatts of net laser beam power. The general configuration arrangement is shown in Figure 3.3-3.

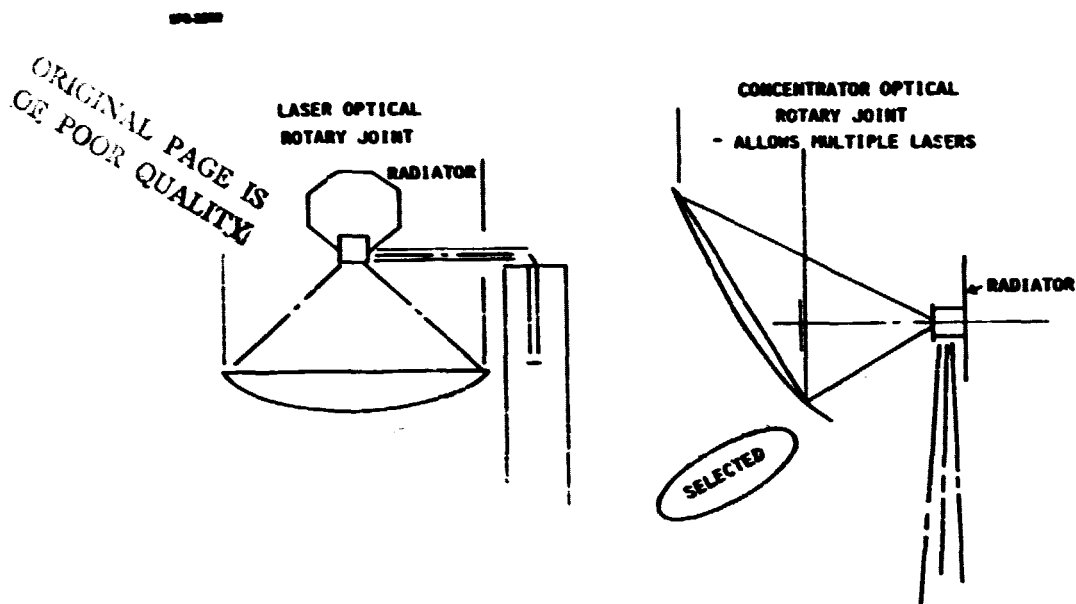


Figure 3.3-2: IOPL Optical Rotary Joint Trade

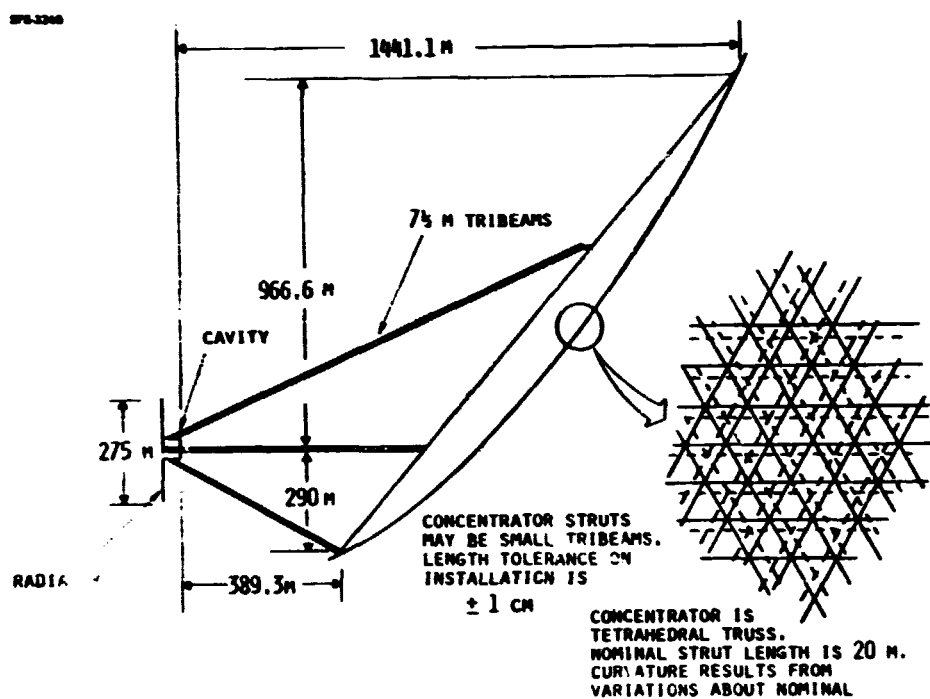


Figure 3.3-3: Indirectly Optically Pumped Laser SPS General Arrangement

### Concentrator Geometry

The off-axis concentrator consists of that segment of a paraboloidal surface within a right circular light cone extending from the cavity. The concentration of sunlight increases with the cone half-angle, as does the amount of sunlight intercepted by a concentrator of given focal length. The concentration ratio affects the maximum temperature that can be achieved in the cavity. This occurs because the cavity views the concentrated solar image and cold space. As the cone angle becomes larger, the solar image view factor and the attainable temperature increase, as shown in Figure 3.3-4. The heat input to the cavity may be expressed as an adiabatic temperature. I.e. with no heat withdrawn, the cavity will reach a temperature such that the heat reradiated equals the heat input. The actual cavity temperature will be less according to the amount of heat withdrawn. The cavity will reradiate heat at its actual temperature; the efficiency with respect to reradiation can be expressed in terms of the ratio of these temperatures as shown in Figure 3.3-5. These figures apply to an ideal concentrator and cavity. The actual concentrator will scatter light according to the degree of imperfection relative to the ideal surface.

Prior studies of the indirect optically-pumped laser by Math Sciences Northwest showed a cavity temperature of 1750K to be approximately correct. Referring to the previous figures, a ratio of  $T_w/T_{aw}$  of 0.6 yields an efficiency well in excess of 80%. The value of  $T_{aw}$  should therefore be about 2900K. This requires an ideal concentrator cone angle of 17 degrees. To compensate for concentrator imperfections an angle about twice the ideal should be used; a value of 0.6 radians (34 degrees) was selected.

Figure 3.3-6 shows the concentrator geometry as viewed from sunward. This displays the sunlight intercept area; the computer routine used to generate these plots was also used to integrate the area; area versus cone angle is plotted in Figure 3.3-7. The concentrator geometry as viewed from the side is shown in Figure 3.3-8, for the selected cone angle of 0.6 radians. For similar geometries the concentrator light power scales with focal length squared. Figure 3.3-9 shows the variation of light power with focal length. As was previously mentioned, the concentrator is made up of many independently steered reflector facets similar to those on earlier solar thermal SPS designs. These are illustrated in Figures 3.3-10 and 3.3-11, and meet the requirements in Table 3.3-1.

SPS-3226

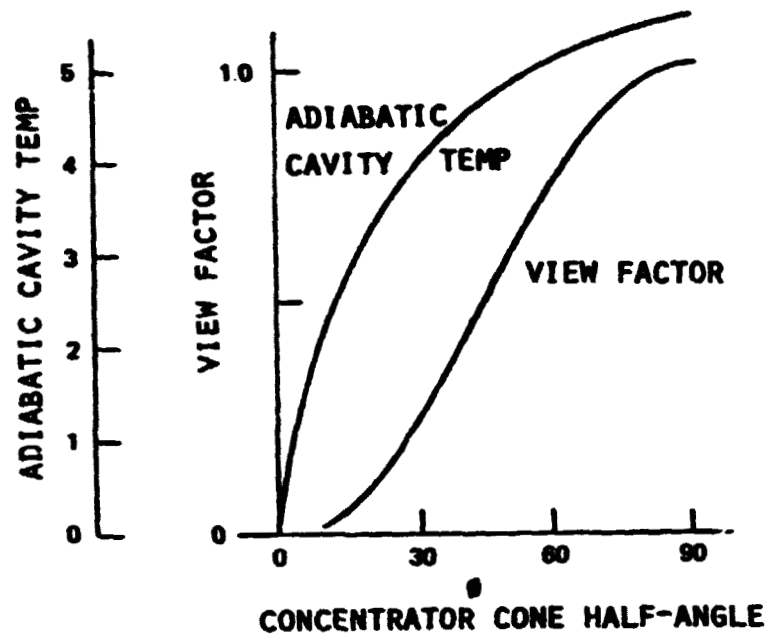


Figure 3.3-4: Cavity Solar Image View Factor and Wall Temperature as a Function of Cone Angle

SPS-3227

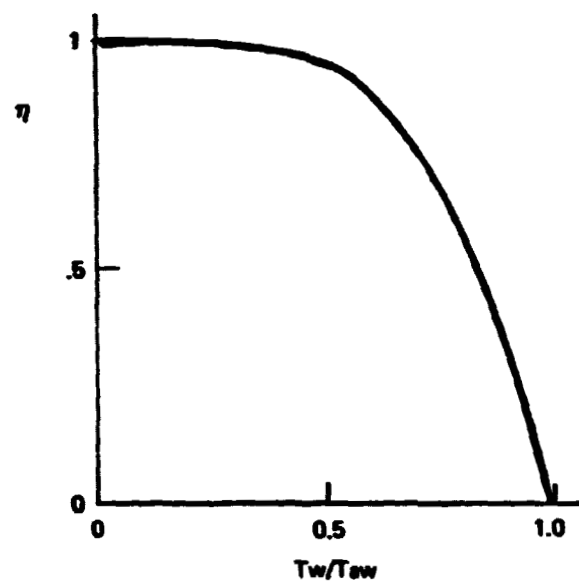


Figure 3.3-5: Ideal Cavity Aeradiation Efficiency

070.0012

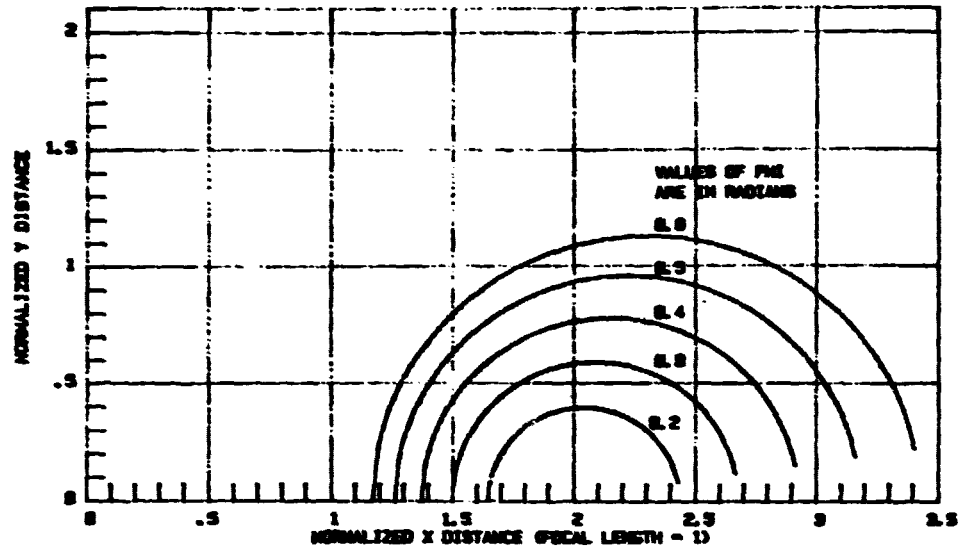


Figure 3.3-6: Reflector Geometry Viewed from Sun Work



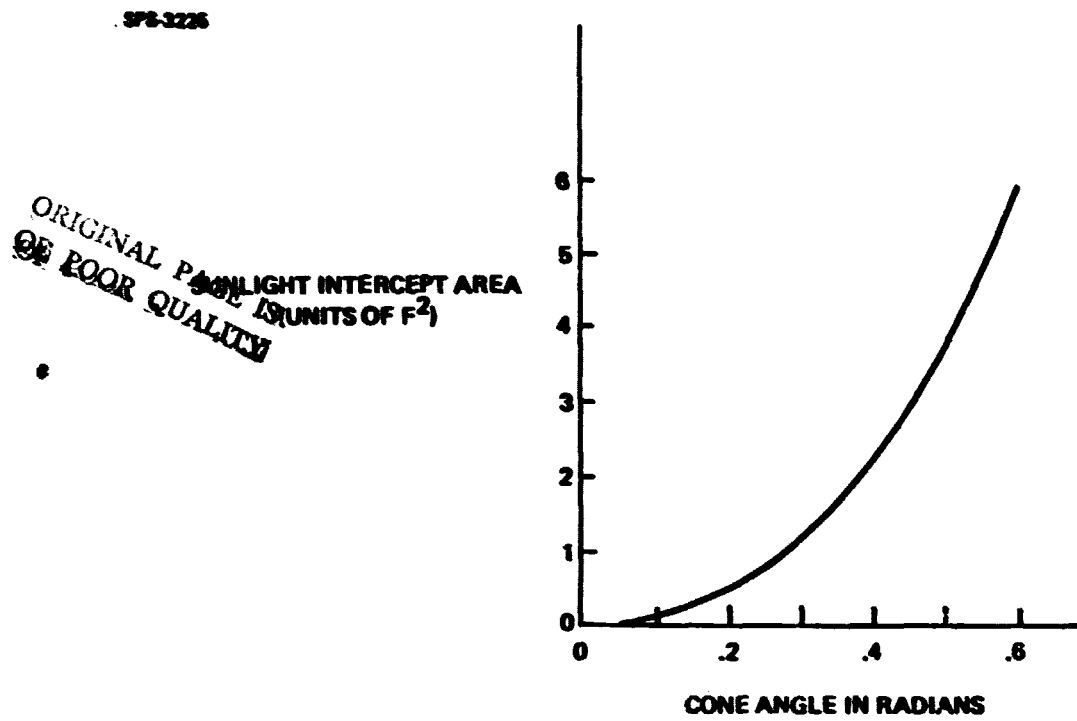


Figure 3.3-7: Concentrator Area

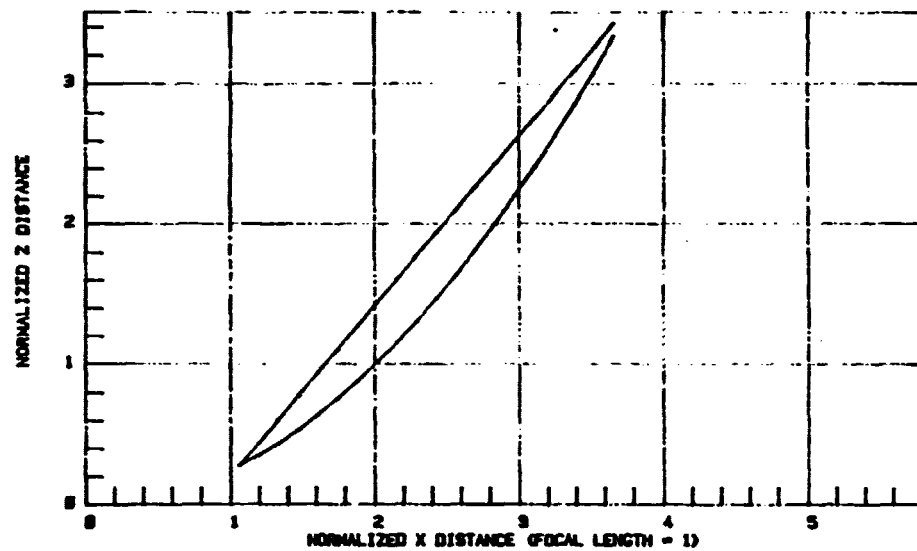


Figure 3.3-8: Concentrator Geometry-Side View

SP-3320

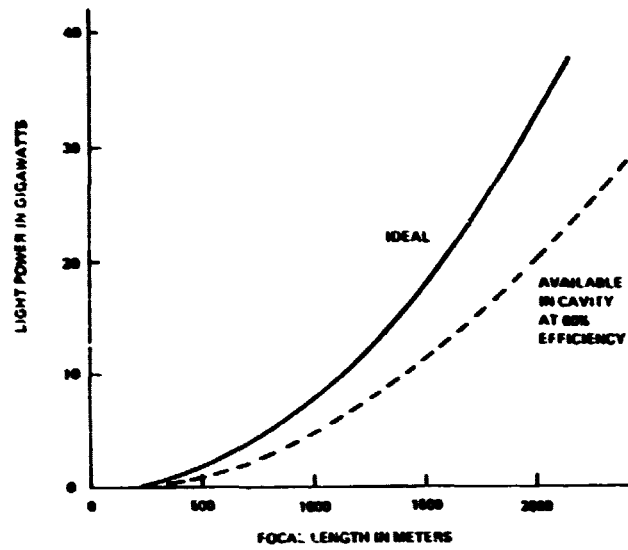


Figure 3.3-9: Light Power and Cavity Thermal Power

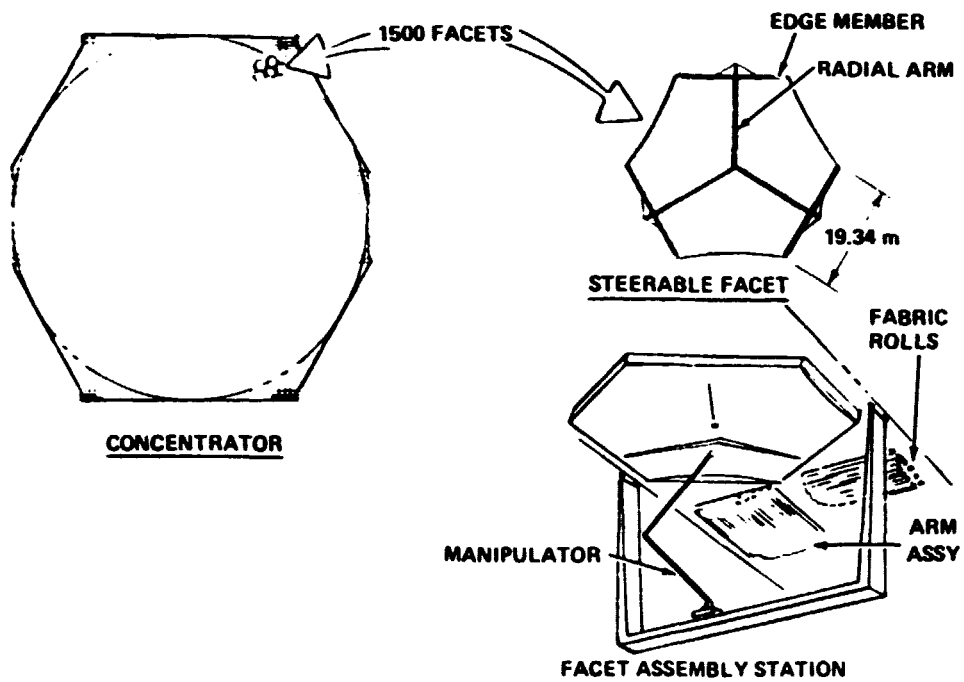


Figure 3.3-10: Concentrator Facets

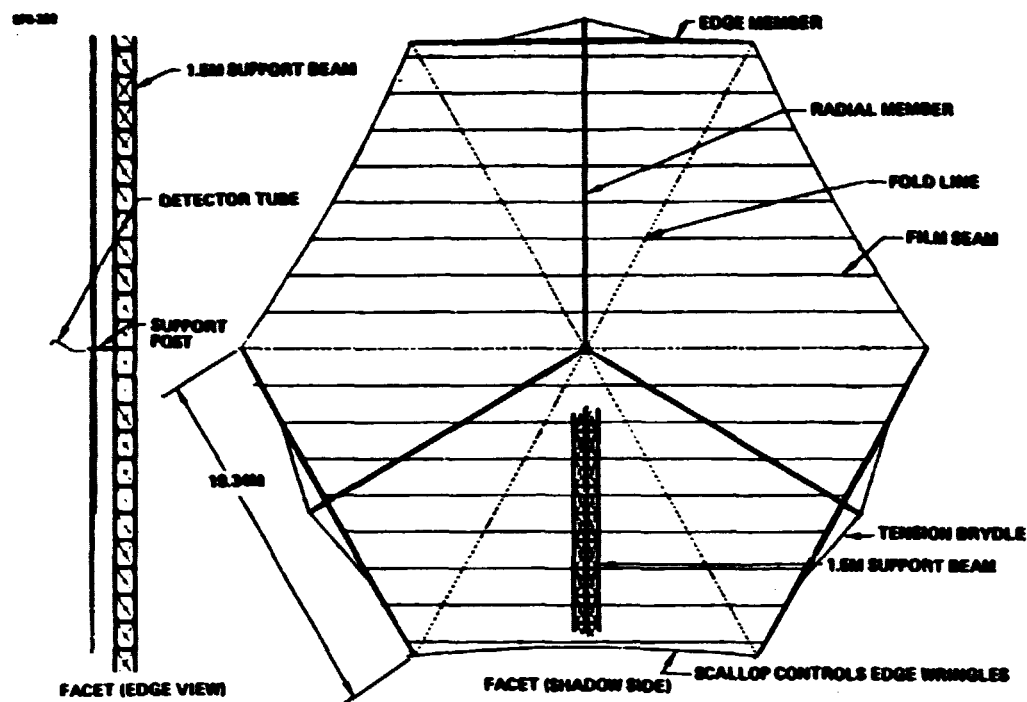


Figure 3.3-11: Reflector Facet Configuration

Table 3.3-1: Solar Pumped Mixing Laser Cycle

- High reflectivity (> 0.80 initial) \*
- Low mass per unit area ( $0.05 \text{ kg/m}^2$ )
- Flat surface
- Accurate pointing ( $\pm 10$  minutes, maximum)
- No calibration required after installation
- Must find "cold" cavity when required
- Must look away from "hot" cavity when required
- Long mean time between failure
- No frame wiring

\*Radiation induced degradation accepted as an oversizing penalty

Due to power scaling problems, the mixing gas laser SPS configuration decided upon has 8 separate 12.5 MW lasers. These each consist of 20 amplifier modules in series using the gas dynamic cycle shown on Figure 3.3-12. The optical pumping is done in 20 pairs of pumping tube modules each covering a 5m x 10m area of the black body cavity surface. (See Figure 3.3-13) There is enough optical gain so that any single amplifier module may be turned off without bringing the chain down. After passing through the amplifier modules the gas is collected and separated via a refrigeration cycle.

The mixing gas IOPL's performance is severely hampered by the necessity to separate the CO<sub>2</sub> lasant from the CO pump gas by refrigeration to the CO<sub>2</sub> liquification temperature. A more appropriate lasant such as an organic compound with a higher liquification temperature would greatly increase system performance by eliminating the substantial refrigerator power penalty.

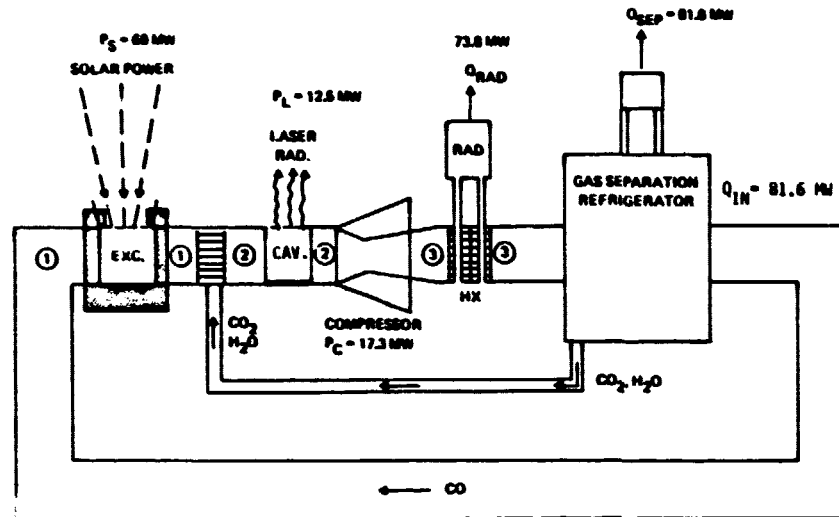
In view of the problems involving both the refrigeration cycle and the constructability of the IOPL SPS, (see Section 5 of this report) further analysis of this system was curtailed and the focus for the most attractive laser SPS candidate was shifted to the free electron laser. This is described in the remainder of this section.

### **3.4 FREE ELECTRON LASERS**

#### **3.4.1 Introduction; The Efficiency Question**

At the beginning of this study, Free Electron Lasers (FEL's) were singled out as being attractive if efficiencies as high as the .5 - .8 claimed possible<sup>1,2</sup> could be achieved. The answer to the efficiency question appears to lie in the fundamental physics of FEL's, and there is a division in opinion on achievable efficiency by the experts in the field (which includes most of the big names in high energy storage rings). However, it is possible to qualitatively describe the aspect of operation of FEL's that (the experts tend to agree) is the key to the efficiency question. This follows.

The first FEL was constructed at Stanford in 1977 by Deacon, et al.<sup>3</sup> Prior to this there were about 10 years of mostly theoretical speculation on FEL's. Also Deacon's group had made some gain measurements in amplification of 10.6 micron CO<sub>2</sub> laser light with basically the same apparatus a year previously.<sup>4</sup>



ORIGINAL PAGE IS  
OF POOR QUALITY

STATE	T <sub>GAS</sub>	T <sub>VIB</sub>
1	400	400
1'	400	1750
2	400	1750
2'	500	950
3	500	550
3'	800	400

Figure 3.3-12: Solar Pumped Mixing Gas Laser Cycle

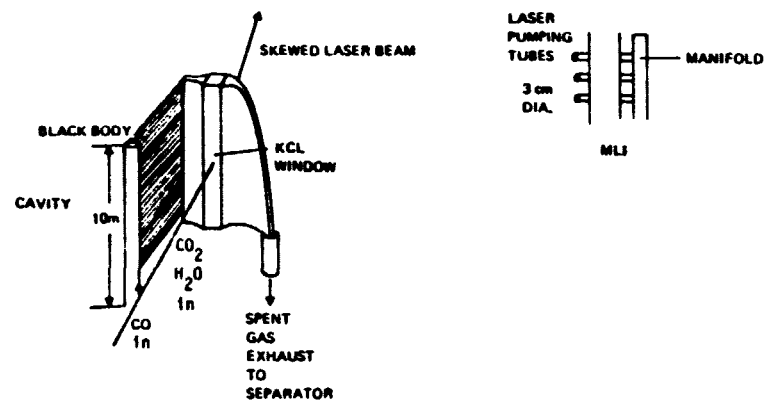


Figure 3.3-13: Laser Amplifier Module Decoys

The first FEL consisted of a 5.2 meter long 160 turn 3.2 cm period 2.4 kilogauss superconducting wiggler magnet with a 43 MeV bunched electron beam passing through the center and two confocal mirrors spaced appropriately so that light from prior electron bunches would interact with successive bunches. Figures 3.4-1 and 3.4-2 (from Ref. 3) illustrate the laser configuration and the emission above and below lasing threshold.

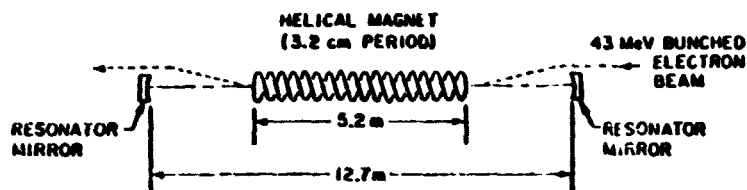
What happens in the FEL is that an initially uniform relativistic electron beam passes through a centimeter scale periodically modulated magnetic field. The magnetic field appears Doppler shifted up to optical frequencies by the electrons, which subsequently take part in a collective stimulated emission process. The consensus of the authorities is that this collective process is basically an electrostatic bunching of the electrons in an approximately parabolic harmonic oscillator potential created by the vector potential of the coincident light beam. If the energy of the electrons is slightly greater than that required to emit at the "natural" frequency of the Doppler shifted static magnetic field, some forward slip of the electron beam with respect to the light wave occurs and energy is coupled into amplification of the light. The reverse can also happen and has been proposed in several laser-electric convertor schemes.

In the process of light amplification, the initially uniform incident electron beam is split and spread in energy well past the slight energy shift due to the slip. (See Figure 3.4-3). The key to whether or not high efficiency due to complete electron beam use and/or reuse is achievable is whether or not this electron beam energy dispersion represents a thermal process or not. If it is a thermal process, it can be shown<sup>5</sup> that only low electron beam power extraction efficiencies are possible. On the other hand, if it is possible to use standard accelerator physics techniques to reform a monoenergetic beam or use a non-uniform wiggler magnet that can operate efficiently with the distorted beam, a high (over 50%) extraction of light energy from the electron beam should be possible.

The consensus of various authorities is that the physics of the beam is classical (as opposed to quantum mechanical) physics much like that of relativistic electron beam tubes that amplify microwaves and millimeter waves. The small signal characteristics of FEL's are understood and agree with experiment. However, the comprehensive large signal and saturation effects understanding that is crucial to answering the efficiency question is not yet at hand, but should be answerable within three years. It is recommended that the existing research activity on large signal behavior of FEL's be monitored for several years it takes the existing FEL community to get the answer.

ORIGINAL PAGE IS  
OF POOR QUALITY

D180-25969-3



$$\lambda = \frac{\lambda_s}{2\gamma^2} \left[ 1 + \frac{1}{4\gamma^2} \left( \frac{\lambda_s^2 r_0 B^2}{mc^2} \right) \right]$$

#### ELECTRON BEAM CHARACTERISTICS

ENERGY	43.5 MeV
WIDTH (FULL WIDTH AT HALF-MAXIMUM):	0.05%
AVERAGE CURRENT	130 $\mu$ A
PEAK CURRENT	2.8 A
EMITTANCE (AT 43.5 MeV):	0.06 mm mrad

Figure 3.4-1: Schematic Diagram of the Free-Electron Laser Oscillator  
(For more details see Ref. 3)

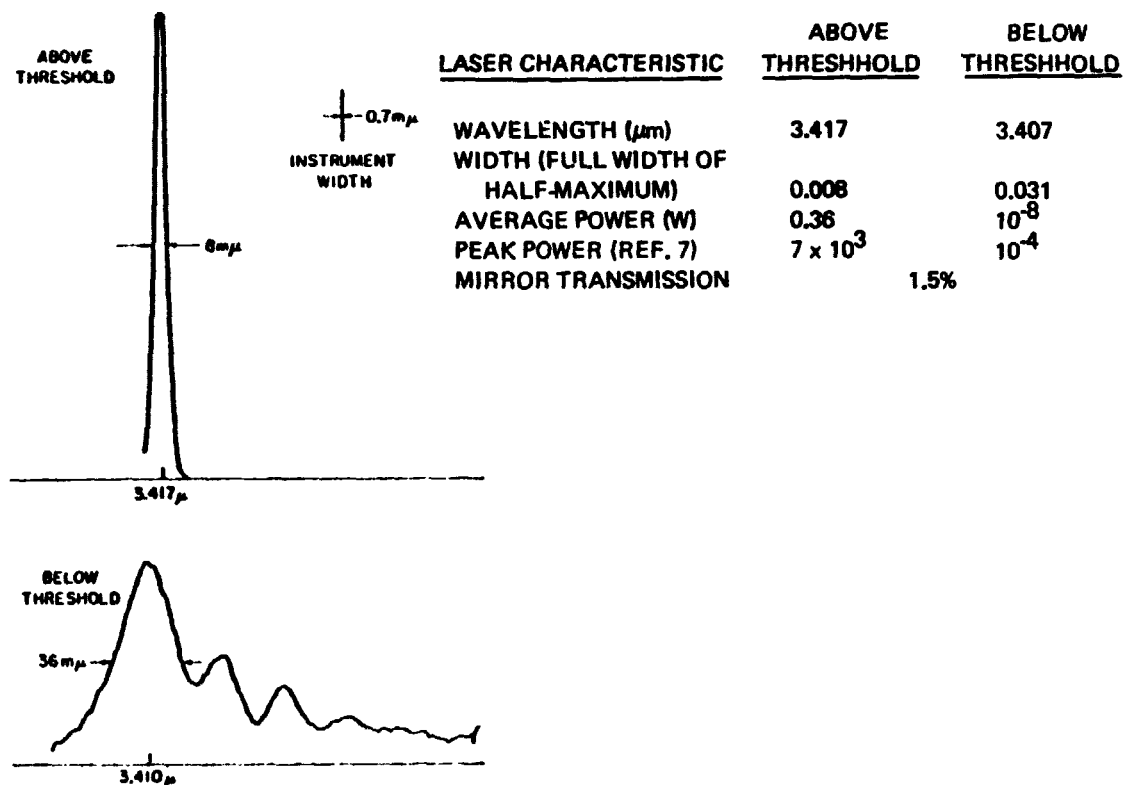


Figure 3.4-1: Emission Spectrum of the Laser Oscillator Above Threshold (Top)  
and of the Spontaneous Radiation Emitted by the Electron Beam (Bottom)  
(From Ref. 3)

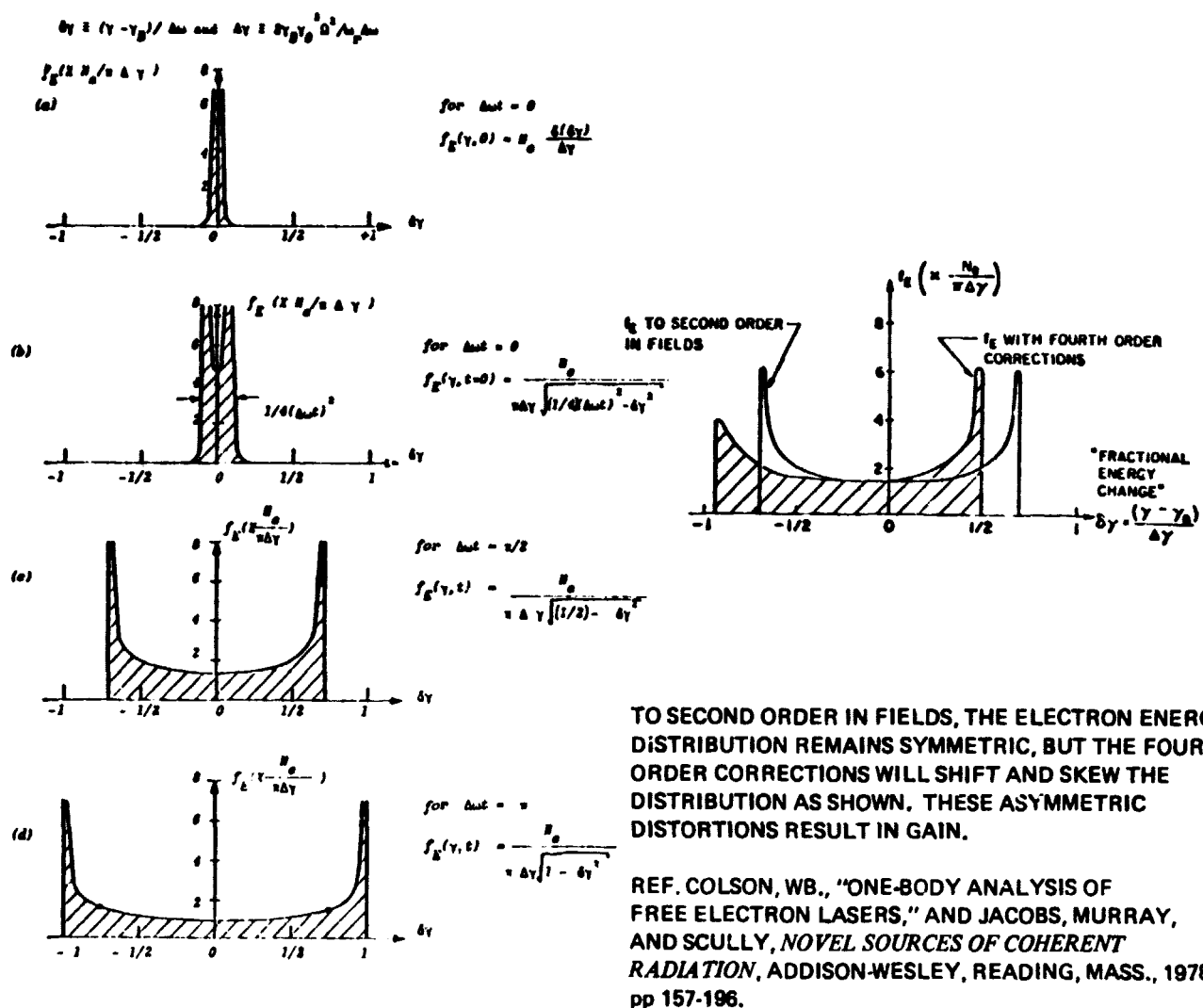


Figure 3.4-3: Evolution of the Electron Energy Distribution as Electrons Pass Through the Laser



We have investigated three possible versions of the free electron laser:

- o CATALEC FEL
- o Double FEL
- o Storage Ring FEL

Each of these is illustrated schematically in Figure 3.4-4. The CATALAC FEL is based on a concept developed at Los Alamos Scientific Laboratory<sup>6</sup> to help recapture some of the electron energy left over at the exit of the laser cavity. These electrons are recirculated through the rf-linac 180° out of phase with the next bunches of electrons to be accelerated. The electrons are decelerated and return most of their remaining energy to the accelerating field. The linac, therefore, behaves as a catalyst for transferring the energy of decelerating electrons to those being accelerated. The spent electrons are dumped at the other end of the linac with approximately 8 MeV, and the accelerated electrons emerge with energies on the order of 50 MeV.

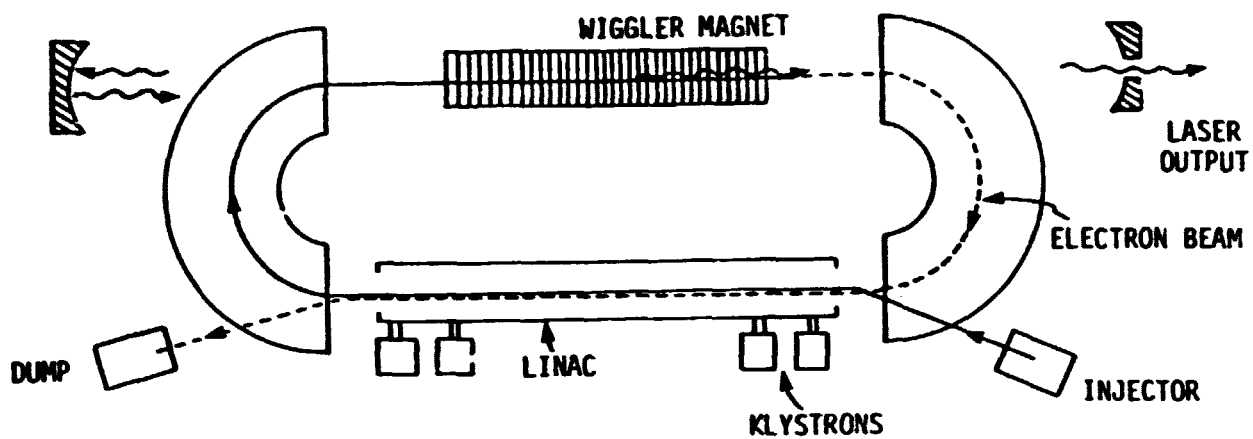
The double FEL uses two electron beams. One beam interacts with a wiggler magnet (on the left) and the other does not.<sup>7</sup> The resulting long wavelength laser radiation produced by the first electron beam is trapped as a standing wave between two mirrors. The standing wave field acts as a virtual wiggler magnet for producing shorter wavelength from a second electron beam (on the right). The advantage of this scheme is to enable lower voltage electron beam sources to be used to produce short wavelength laser radiation. This also makes beam energy recovery for once-through FELs more efficient. However, the submicron wavelengths that this scheme can provide are not desired for SPS power transmission.

The storage ring FEL provides a well tested technology for recirculating the electron beam many times through the wiggler magnet of the FEL.<sup>8</sup> On each pass the energy losses and energy taken out by the laser beam can, theoretically, be replaced by accelerating the electrons in the storage ring with an RF cavity. A technical difficulty with that is that the electron bunches must be phase synchronized with the optical field when they return for each pass. Given the many disturbances that can occur on the recirculation path it is not obvious that this resynchronization will be easy to achieve.

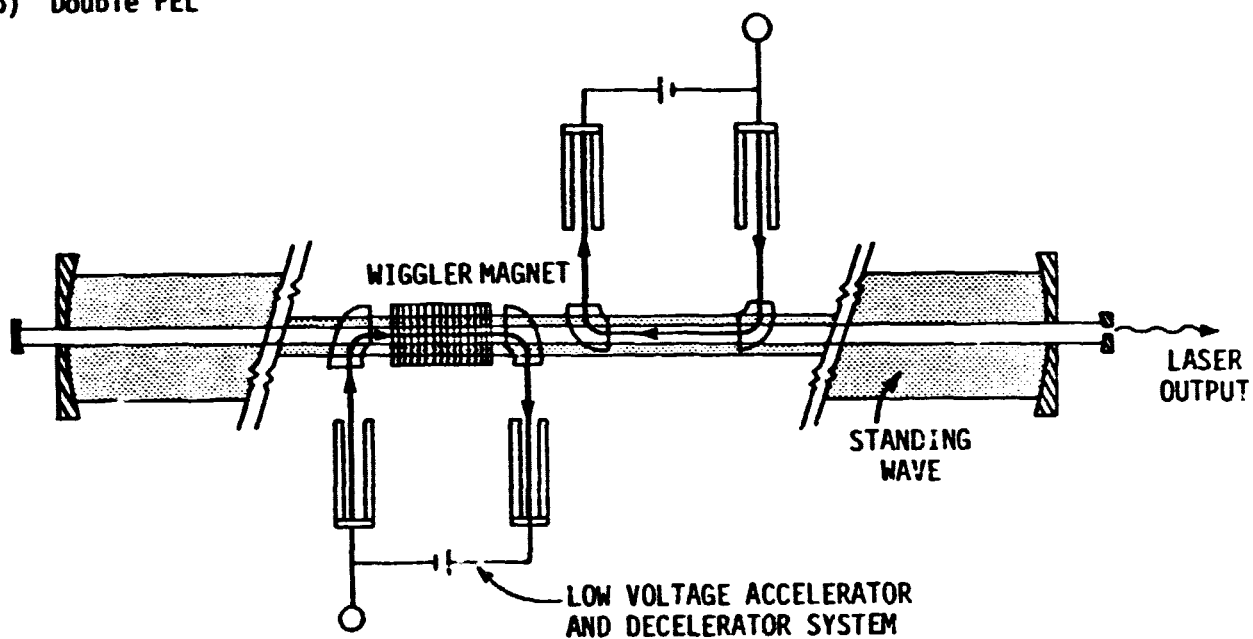
No high power FELs have been built in the wavelength range suitable for atmospheric propagation, so this technology must be regarded as rather tentative. The elementary

(a) CATALAC FEL

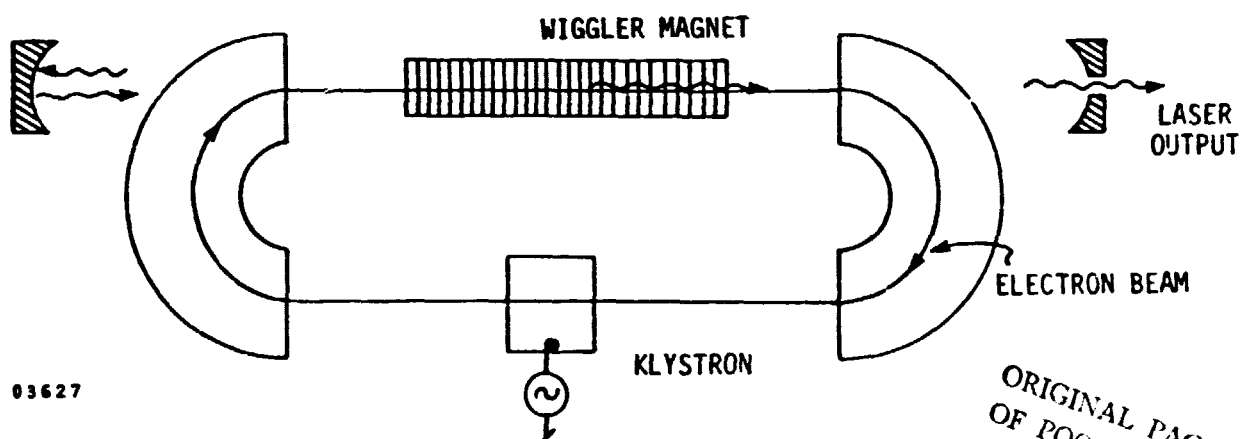
D180-25969-3



(b) Double FEL



(c) Storage Ring FEL



80 03627

Figure 3.4-4: Candidate Free Electron Laser Concepts

ORIGINAL PAGE IS  
OF POOR QUALITY

gain and oscillator experiments that have been performed at Stanford<sup>3</sup> which indicate, in principle, that the laser will work. Several more substantial experiments for 1 micron lasers are now in the planning stage and are due to come on line in late 1980 or 1981.<sup>9</sup>

Nevertheless, a substantial amount of theoretical analysis has been performed which permits elementary scaling calculations; the results of these are included in Table 3.4-1 for the CATALAC FEL. This operates essentially as a once-through device with good energy recovery. We have chosen this device over the other two concepts because the storage ring FEL has the unresolved problem of how to rebunch the electron beam emerging from the wiggler so that it will be capable of full resonance when it re-enters the wiggler for the next pass through. The double FEL is at present too sensitive to the assumption of low losses of the standing EM wave (i.e., virtual wiggler field) to be considered at this point.

### 3.4.2 FEL Design Considerations

Once-through, high extraction lasers appear to be the most practical FEL lasers at present. We have examined this case with energy recovery from the spent electron beam (i.e., the CATALAC) where the extraction is on the order of 20 percent as well as higher extraction (up to 50 percent) with no electron beam energy recovery.

The governing equations are those which determine the resonance between electrons and photons and the energy equation for free electrons

$$\gamma^2 = \frac{\gamma_m}{2\gamma_p} (1 + a_w^2) \quad (1)$$

$$\frac{d\gamma}{dz} = \frac{-e_s a_w}{\gamma} \sin \psi \quad (2)$$

where  $a_w = \frac{eB\gamma_m}{2\pi mc^2}$  and the constant of motion,

$$\frac{CE_0^2}{4\pi} + \frac{j\gamma mc^2}{e} = \text{Const.} \quad (3)$$

By integrating the equation of motion over a confocal length for the photon beam, one can obtain an implicit equation for the ratio of the photon beam power to electron beam power which is accurate for large extractions (i.e., large  $\frac{\Delta\gamma}{\gamma_i}$ ). The resulting equation is

$$\left(3 + 2 \frac{P_p}{P_B} - \frac{\Delta Y}{Y_i}\right) \left(\frac{P_p}{P_B} + \frac{\Delta Y}{Y_i}\right)^{\frac{1}{2}} - \left(3 + 2 \frac{P_p}{P_B}\right) \left(\frac{P_p}{P_B}\right)^{\frac{1}{2}} = 2 \times 10^{-4} (\sin \psi) H \frac{a}{\lambda_m} (P_B)^{\frac{1}{2}} \quad (4)$$

where  $\psi$  = synchronous phase angle  
 $P_p$  = input optical power  
 $P_B$  = input e-beam power  
 $H$  = product of the electron capture fraction and the E field radial shape factor  $\langle E(r) \rangle / E(r=0)$   
 $a$  = outer radius of the photon beam

This equation has been solved for  $\frac{\Delta Y}{Y_i} \approx 0.2$  and  $\frac{\Delta Y}{Y_i} \approx 0.5$ , assuming  $H = 0.5$ ,  $\sin \psi = 0.5$ ,  $a = 1$  cm and  $\lambda_m = 6$  cm.

Because the electron beam is accelerated by klystrons, it arrives at the entrance to the wiggler magnet already bunched; further bunching occurs when the FEL operates in a saturated mode since the electron bunches oscillate within the potential wells of the growing electromagnetic wave. Considering the duty cycle of the macroscopic current to be 0.01 and the duty cycle of micropulse (caused by bunching in the wiggler magnet) to be approximately  $2.5 \times 10^{-2}$ , the instantaneous laser power is 4 GW. The corresponding initial electron beam power is 22 GW. The gain for this laser is  $2.05 \times 10^3$  which means that the input laser beam has an average intensity of 488 Watts. The exiting electron beam power is reduced to 17.6 GW.

In order to maintain resonance between the electron beam and the laser beam, the resonance condition requires that the spacing between the wiggler magnet decrease; holding the laser wavelength constant, the spacing at the wiggler magnet exit will be 3.5 cm instead of 6 cm.

The preceding calculation assume that  $a_w = 1$  optimization is maintained over the length of the wiggler magnet. This requires an increase in wiggler field strength at the beam exit end since  $\lambda_m$  is decreasing. The dependence of  $a_w$  on magnet current and spacing is

$$a_w = 1 e^{-r/\lambda_m} \quad (5)$$

where  $r$  is the radius of the magnet bore and  $I$  is the current. For modest extractions (i.e., up to 30 percent)  $a_w = 1$  is a reasonable assumption. However, for 50 percent extraction or greater, the magnet spacing goes to 1.5 cm unless  $a_w$  is allowed to vary. Thus, to maintain an acceptable magnet spacing (i.e., larger than the magnet bore radius), we propose increasing  $a_w$  towards the exit. To a certain extent this strategy reduces the extraction which could otherwise be obtained but it keeps the current needed to drive the magnets within bounds.

Table 3.4-1 summarizes the basic relationships describing the FEL parameters once the gain, extraction, and magnet separation ( $\lambda_m$ ) are known. Several parameters are free to be chosen. In particular, the laser wavelength  $\lambda_p$  can be chosen and a fill factor relating the photon beam waist radius to the electron beam (magnet bore) waist radius needs to be prescribed. For purposes of illustration, the fill factor is taken to be 1 (i.e.,  $a = r$ ) and  $\lambda_p = 5$  microns.

The efficiency of the FEL can be estimated for a once-through device in terms of the extraction, the efficiency in accelerating the electrons, and the solar-to-electric conversion efficiency

$$\eta_L = \frac{\Delta \gamma}{\gamma_i} \eta_{KLy} \eta_e$$

Typical values for  $\eta_{KLy}$  are 0.50 (Klystrons and waveguides) to 0.90 (Gyrocons), and  $\eta_e = 0.15$  (photocells) to 0.25 (solar thermal power). Thus, at the upper end of efficiencies

$$\eta_L = .045 \text{ to } .113$$

as the extraction ranges from .2 to .5 .

With energy recovery these values may be raised. The crudest type of energy recovery is to operate the electron beam dump at temperatures approaching the working fluid temperature of the solar thermal power system. Then, total laser efficiency ranges from .055 to .127 for the same range of extractions.

Note that thermal dumping represents a severe penalty in electron beam energy availability from 45 MeV at the exit end of the wiggler. Brau and his associates have proposed an elegant scheme called the CATALAC FEL for using these spent electrons to

Table 3.4-1 a: Example Parameters for a 1 MW Catalec FEL

$\frac{\Delta\gamma}{\gamma}$ (%)	20%	50%
$P_{Bi}$ (Watts)	$4 \times 10^{10}$	$4.75 \times 10^{10}$
$B_i$ (kG) = $10.7 \lambda_{mi}^{-1}$ (cm)	1.78	1.78
$\gamma_i = (\lambda_{mi} \lambda_p^{-1})^{\frac{1}{2}}$	109.5	109.5
$\lambda_{mf}$ (cm) = $\lambda_{mi} (1 - \frac{\Delta\gamma}{\gamma})^2$	3.84	1.50
$\gamma_f = (\lambda_{mf} \lambda_p^{-1})^{\frac{1}{2}}$	87.6	54.8
$B_f$ (kG) = $10.7 \lambda_{mf}^{-1}$ (cm)	2.79	7.13
$L$ (m) = $\lambda_p^{-1} (\pi r^2)$	63	63
$\epsilon_{Bi}$ (MeV) = $0.51 \gamma_i$	55.9	55.9
$I_B$ (A) = $P_B$ (MW) $\epsilon_B^{-1}$ (MeV) $\cdot_{mp}$	7.2	8.5
$n_B$ (cm <sup>-3</sup> ) = $I_B (\pi r^2 e c)^{-1}$	$4.8 \times 10$	$5.4 \times 10^{10}$
$N = L (\lambda_{mi}^{-1} + \lambda_{mf}^{-1}) 0.5$	1345	2625
$\frac{\Delta\gamma}{\gamma} = (2N)^{-1}$	$4 \times 10^{-4}$	$2 \times 10^{-4}$
$P_{pi}$ (MW)	4	475
Gain	$2 \times 10^3$	51
$P_{pf}$ (MW)	$8.2 \times 10^3$	$2.4 \times 10^4$
$P_{av}$ (MW)	2 MW	6 MW

---


$$\tau_D = 0.01$$

$$\lambda_{mi} = 6 \text{ cm}$$

$$\lambda_p = 5 \times 10^{-4} \text{ cm}$$

$$P_{av} = 2.5 \times 10^{-2} \tau_D P_{pf}$$

Subscripts i,f refer to initial and final (i.e., output).

Table 3.4-1 b: Example Parameters for a 1 MW Catalec FEL

Laser and Wiggler Magnet

$\lambda_L = 5\mu$ , laser wavelength

$P_L = 1$  MW, laser output power

$\lambda_m = 6$  cm, wiggler period

$L_m = 163$  m, wiggler length

$B_m = 1.8$  kGauss, field strength

$\frac{\Delta\nu}{\nu} = 2 \times 10^{-4}$ , laser line width

$G = 2 \times 10^3$ , Gain

$\left(\frac{\Delta Y}{Y}\right) = 18\%$ , Extraction

$D_L = 571$  m, optical intercavity distance

$r_L = 1.61$  cm, optical waist radius

Storage Ring

$r_R = 10$  m, turning radius

$B_R = 222$  Gauss

$\sigma_R = 0.02$  mm, radial spread

$\sigma_Z = 2 \times 10^{-4}$  mm, vertical spread

Electron Beam

$\gamma_B = 109.5$ , relativistic gamma

$E_B = 55.9$  MeV, electron energy

$I_B = 10$  A, average current

$n_B = 1 \times 10^{10}$  elect/cm<sup>3</sup>, electron density

$P_B = 5.60$  MW, average power

$r_B = 1.0$  cm, electron beam waist in wiggler

$L_B = 4$  cm, electron beam microbunch length

$\tau_B = 133$  ps, microbunch period

$\tau_{BR} = 5.2$  ns, microbunch repetition period

$\tau_m \equiv \tau_{BD} = 2.56 \times 10^{-2}$ , e-beam current duty cycle in microbunch

$I_{peak} = 0.391$  kA =  $\tau_{BD}^{-1} I_B$

$\epsilon_B \leq \pi$  0.9 mm mrad, emittance limit on e-beam

D180-25969-3

**Table 3.4-1 c: Example Parameters for a 1 MW Catalac FEL**

<u>Injector</u>	<u>Klystrons</u>
$\eta_I = 50\%$ , wall-plug	$V_K = 300$ keV, voltage
$\epsilon_I = 10$ MeV	$\omega_K = 67$ MHz, frequency
$I_I = 10$ A per pulse	$P_K = 500$ kW, power
$\tau_I = 100$ $\mu$ sec, (Klystron pulse length)	$\eta_K = 50 \sim 90\%$ , wall-plug
$\tau_D = 0.01$ , Injector Duty Cycle	



accelerate a new chain of electron bunches to 55.9 MeV. As described previously the spent electrons are captured with turning magnets and reinjected  $180^\circ$  out of phase into the linear accelerator. Here they give up their energy by slowing down in the wave frame of the accelerating field and exit the other end of this "catalyzed" linac at energies very close to the energies at which fresh electron bunches are being injected into the system (e.g., 10 MeV).

The CATALAC FEL has the advantage of allowing a much less energetic injector to be used; for example, cold cathode pulsed e-beam technology can reach 10 MeV without difficulty; similarly, a device called a microtron could also be used. Of course, the full linac klystron power must be turned on to start the laser, but once the first group of electrons have passed through then the accelerating field will be largely sustained (except for losses in the linac) by the electrons themselves. Hence, the weight of the laser itself will not be reduced by this design, but the solar array or thermal power system can be substantially reduced if suitable start-up energy storage is available. Not much energy is required for this storage since the start-up is accomplished very rapidly; hence, the storage weight should be negligible.

Table 3.4-1 shows point design values for a 1 MW CATALAC FEL for an extraction of 18 percent. If we assume that the only losses from the system are the 10 MeV spent electron beam (with no recovery), or a total power loss of  $\tau_{DI} I_e \epsilon_1 = 0.01 (10A) 10MeV = MW$ , then the effective "extraction" efficiency is

$$\eta_{ext} = P_L (P_L + P_{Loss})^{-1} \approx .5$$

regardless of the actual per-pass extraction efficiency. With recovery of the beam dump as before we can expect overall laser efficiencies in the 12 percent range, even for single pass extraction substantially less than 50 percent.

The FEL concept appears to scale to much higher power outputs per module with no special constraints from the laser cavity. However, because of the high intensity nature of the laser beam (e.g., gigawatts/cm<sup>2</sup>), the laser optics are a serious problem. Either the cavity mirrors (in the case of an oscillator) and/or the expansion optics must be removed quite some distance from the active laser medium. In contrast to gas lasers, this poses no immediate problem for the FEL since the laser medium need not be enclosed over the intercavity length between optical elements; indeed, the hard vacuum of space is an ideal

environment for FEL cavity operation. As one approaches gigawatt average power levels, the intercavity distance reaches 18 km. The use of glancing angle optics may be a useful way to reduce the unit area radiant power loading and keep the intercavity distance within bounds.

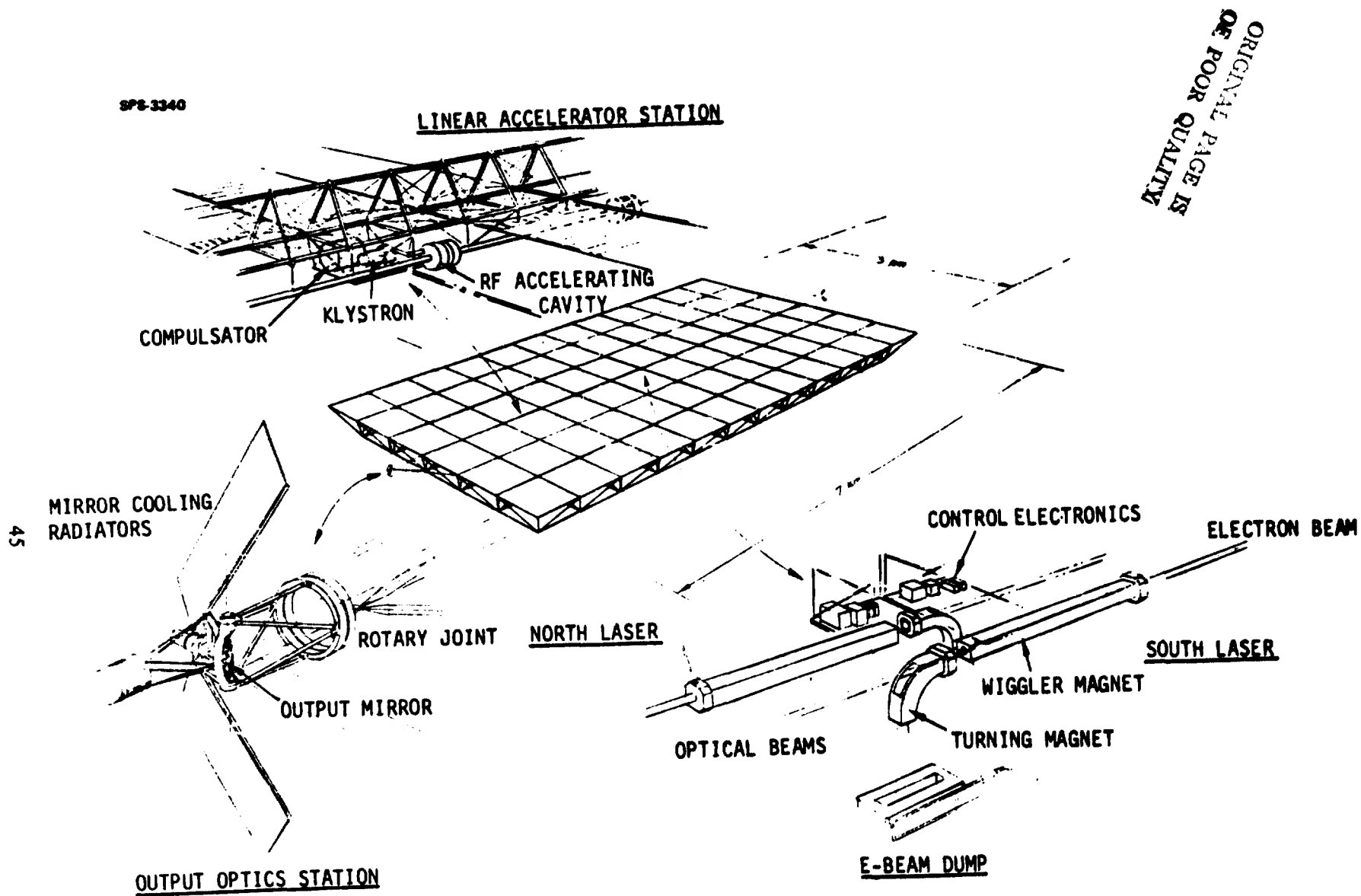
### 3.4.3 Single Pass FEL SPS

A single-pass FEL SPS which produces 1 GW of grid power using two .5 GW downlink beams was configured as shown in Figure 3.4-5, with two linear electron beam accelerators along the spine of a 7 km long x 3 km wide photovoltaic satellite. The electron beams originate from cathode stations at each end of the satellite spine and are accelerated by approximately 330 klystron/RF accelerator stations located every 10 meters along the line. The main portion of the lasers, the wiggler magnets, are located on two pairs of 5m x 5m pallets at the satellite center. After passing through the wiggler with 50% extraction, the beam is magnetically turned into the plane of the satellite and dumped in a small 700K radiator located in the shade behind the back of the solar array. The laser light beam is of course not bent by the magnet and continues straight along the spine increasing in diameter from its original 1 cm dimension by diffraction as it does so. At the end of the satellite it encounters the actively cooled and controlled output mirror which deflects the now 3 meter beam towards the receiving site on earth.

Tables 3.4-2 through 3.4-4 give efficiency, mass and cost estimates for this configuration. The mass per unit delivered power is roughly twice that of the microwave reference but the cost (at \$48 a system) is only 2/3 as much because of the lower ground receiver costs. Aside from obvious differences such as different extraction efficiencies the other FEL configurations considered have essentially the same performance as the auxiliary gear of turning magnet and/or more sophisticated control equipment is relatively low in mass.

### 3.4.4 Multiple Pass FEL SPS

It may turn out that the physics of FEL's does not allow the 50% single pass extraction postulated for the satellite above. In this case it is advantageous to recycle the beam a number of passes before discarding it. This is different from the "energy recycling" as done with the Catalac FEL because here the electron bunches are simply circulated N times with no attempt at using interbunch electric potentials like the Catalac does. This might be done with the minimal mass penalty of several turning magnets, some control electronics and some more sophisticated power processing equipment.



D180-25969-3

Figure 3.4-5: 1 GW Single-Pass Free Electron Laser SPS

Table 3.4-2: Single Pass Free-Electron Laser Efficiency Estimate

<u>EFFICIENCY ESTIMATE</u>		
<u>POWER</u>	<u>AT</u>	<u>EFFICIENCY</u>
1 GW	GROUND	
1.25 GW	ON RCVR	.80 IR/ELECTRICITY
1.3158	INTO ATM	.95
2.6315	E-BEAM	.50 E-BEAM/LIGHT
3.289	EL. PWR	.8 ELEC./E-BEAM
3.46	ARRAY OUTPUT	.95 UNCONDITIONED-CONDITIONED POWER
24.73	SUNLIGHT	.14 SUNLIGHT-UNCONDITIONED ELEC.
- 4% vs 7% FOR MICROWAVE		

Table 3.4-3: Single Pass Free Electron Laser Mass Estimate

<u>MASS ESTIMATE</u>			
<u>ITEM</u>	<u>FACTOR</u>	<u>BASIS</u>	<u>ESTIMATE (MT)</u>
COOLING SYSTEM	3 KG/KW <sub>TH</sub>	100 KW <sub>TH</sub>	30
LASER & CAVITY OPTICS	0.1 KG/KW <sub>L</sub>		100
RADIATOR & COOLING	0.4 KG/KW <sub>TH</sub>	1.3 x 10 <sup>6</sup> KW <sub>TH</sub>	520
HOUSING & MOUNTING	25%		160
KLYSTRONS & E-OPTICS	1 KG/KW <sub>E</sub>	3.289 x 10 <sup>6</sup> KW <sub>E</sub>	3,289
POWER PROCESSING	2 KG/KW <sub>E</sub> & 15%	3.280 x 10 <sup>6</sup> KW <sub>E</sub>	987
POWER CONDUCTORS	0.125 KG/KW <sub>E</sub>	3.289 x 10 <sup>6</sup> KW <sub>E</sub>	411
SOLAR ARRAY	3.3 KB/KW <sub>E</sub>	3.46 x 10 <sup>6</sup> KW <sub>E</sub>	11,418
STRUCTURES	19 KM <sup>2</sup>	19/50 REF	1,768
INFO MGMT & COMM	215 x REF	100	40
ATT. CONTROL	1/10 x REF	212	21
			18,744
RAW TOTAL GROWTH	22%		4,124
TOTAL			<u>22,868</u>

**Table 3.4-4: Single Pass FEL Preliminary Cost Estimate**

<b><u>ITEM</u></b>	<b><u>FACTOR</u></b>	<b><u>BASIS</u></b>	<b><u>ESTIMATE (\$M)</u></b>
OPTICS COOLING SYSTEM	\$100 kg <sup>-1</sup>	30 MT	6
LASER & CAVITY OPTICS	\$200/m <sup>2</sup>	40 m <sup>2</sup>	80
RADIATOR & COOLING	\$150 kg <sup>-1</sup>	520 MT	78
HOUSING & MOUNTING	\$100 m <sup>-1</sup>	160 MT	16
KLYSTRONS & E-OPTICS	\$100 kg <sup>-1</sup>	3,289 MT	329
POWER PROCESSING	\$100 kg <sup>-1</sup>	987 MT	99
POWER CONDUCTORS	\$80 kg <sup>-1</sup>	411 MT	25
SOLAR ARRAY	\$40 m <sup>-2</sup>	1.933 x 10 <sup>7</sup> m <sup>2</sup>	773
STRUCTURES	\$80 kg <sup>-1</sup>	1,768 MT	141
INFO MGMT & COMM	2/5 x REF.	\$48 n	20
ATTITUDE CONTROL	1/10 x REF.	\$160 n	16
RAW TOTAL			1583
GROWTH	17%		269
GROWTH TOTAL	9.56%		1,852
LESS EXPLICIT AMORTIZATION	10%		-177
CONSTRUCTION			185
TRANSPORTATION	(1.05) x \$80 kg <sup>-1</sup>	-22,868 nT	1,441
GROUND RECEIVER	\$1,000 m <sup>-2</sup>	6 x 10 <sup>5</sup> m <sup>2</sup>	600
MGMT, CONTROL, MISC.	1/5 REF.	\$100 m	100
TOTAL DIRECT OUTLAY			4,001

A typical configuration and beam layout might be like the one shown on Figure 3.4-6. Like the previous satellite it has two electron beams providing .5 Gw each on the ground and has a 3 km x 7 km solar array. The electron beam is directed by a switching magnet to separate lasers that are used to extract the beam power at each pass. This allows the lasers to be tailored to the electron beam distributor available at each pass so as to provide highest extraction.

Some parametric curves of electric-to-laser efficiency as a function of extraction acceleration efficiency and number of passes have been developed and are shown on Figure 3.4-7. They indicate that, with a constant 80% acceleration (klystron) efficiency (the same as for the single pass satellite) an extraction of only .2 would yield an electric-to-laser efficiency of .435 with 9 passes, out of an ideal electric-to-laser efficiency of around .45. With the almost certainty achievable extraction of .1 the electric-to-laser efficiency drops to .28 at 12 passes, and with an extraction of .3 it is up to .54 after 8 passes.

Not unsurprisingly, the changes in overall electric-to-laser efficiency are very sensitive to the accelerator efficiency. For instance, with a single-pass extraction of .2 a mere 5% increase in acceleration efficiency to 85% allows a laser that converts 52.5% of its electricity to light after 12 passes.

A caveat regarding the use of these efficiency curves is in order. The constant extraction and constant acceleration efficiency are both extremely naive. It is recognized that in the real case the extraction and acceleration efficiency will vary with pass number. The results above are merely engineering illustrations of the technical implications for various values of the variables involved.

Having to make a number of passes with the electron beams in order to achieve reasonable electric-to-light efficiency necessarily greatly increases the complexity of the electron beam control system. Not only must the electron bunch traffic be handled, but the accelerating devices must be throttled down at each pass as they pump an ever smaller bunch of useful electrons. The mass penalty of this control process is likely to be a small fraction of the system mass but the control system cost may be significant. Also, as the laser is no longer emitting constant intensity light pulses the efficient micro-rectenna receiver concept can not be used to maximum advantage. Thus, multiple pass systems are not recommended for use if high single pass extraction is possible.

ORIGINAL PAGE IS  
OF POOR QUALITY

D180-25969-3

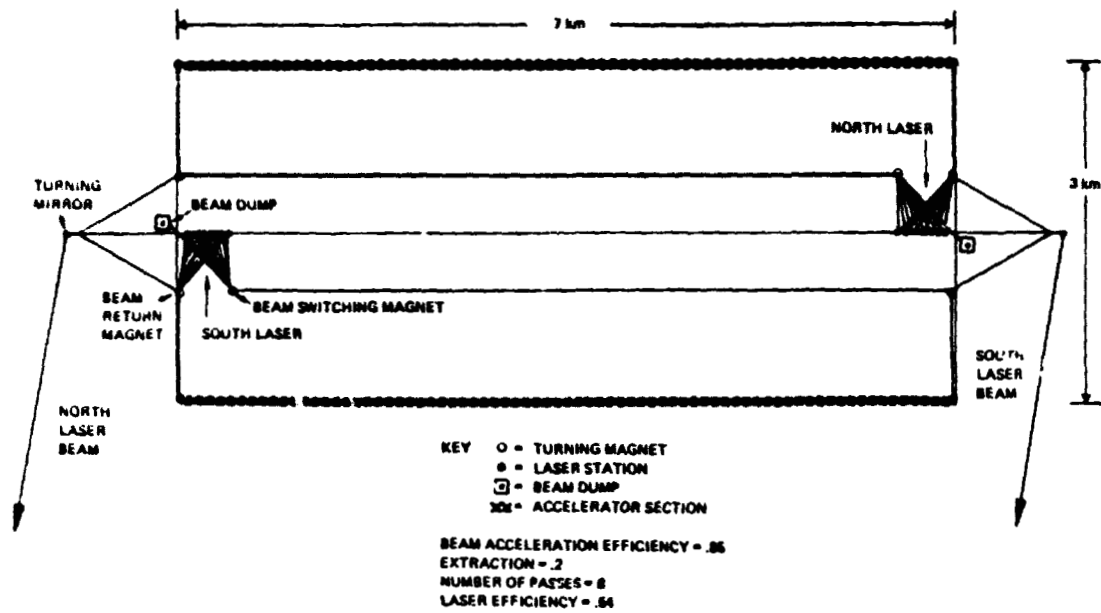


Figure 3.4-6: Multiple Pass FEL Satellite Beam Scheme

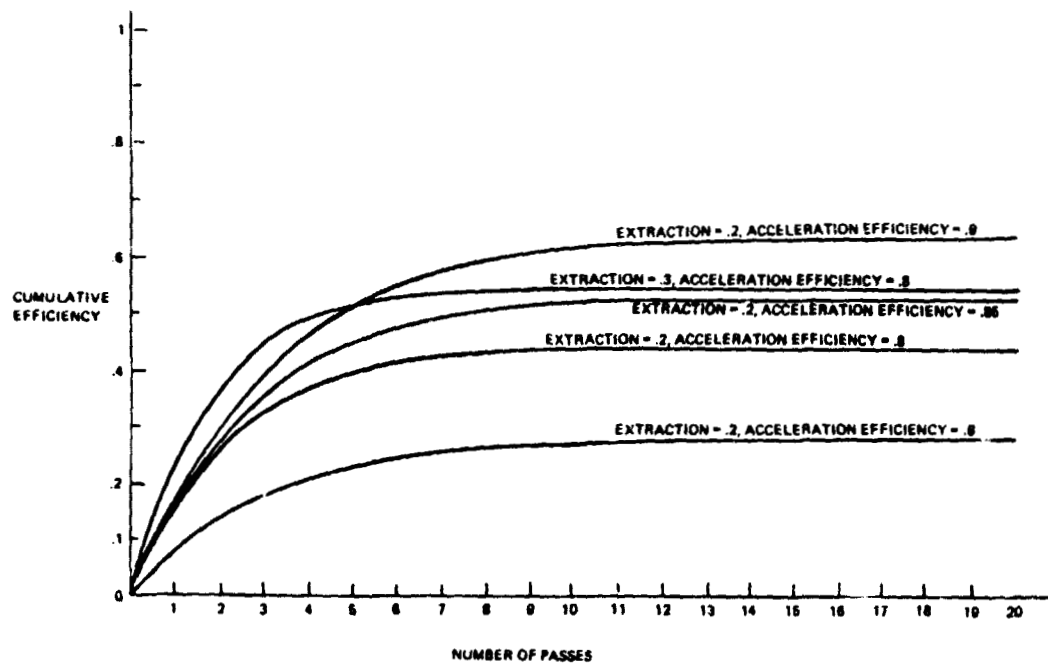


Figure 3.4-7: Multiple Pass Free Electron Laser Efficiencies

increase in acceleration efficiency to 85% allows a laser that converts 52.5% of its electricity to light after 12 passes.

A caveat regarding the use of these efficiency curves is in order. The constant extraction and constant acceleration efficiency are both extremely naive. It is recognized that in the real case the extraction and acceleration efficiency will vary with pass number. The results above are merely engineering illustrations of the technical implications for various values of the variables involved.

Having to make a number of passes with the electron beams in order to achieve reasonable electric-to-light efficiency necessarily greatly increases the complexity of the electron beam control system. Not only must the electron bunch traffic be handled, but the accelerating devices must be throttled down at each pass as they pump an ever smaller bunch of useful electrons. The mass penalty of this control process is likely to be a small fraction of the system mass but the control system cost may be significant. Also, as the laser is no longer emitting constant intensity light pulses the efficient micro-rectenna receiver concept can not be used to maximum advantage. Thus, multiple pass systems are not recommended for use if high single pass extraction is possible.



**3.4.5 Section 3.4 References**

- 1) Deacon and Madey, Physical Review Letters 44, 449-452 (Feb. 18, 1980)
- 2) Lin and Dawson, Physical Review Letters 42, 1670-1673 (June 18, 1979)
- 3) Deacon, Elias, Madey, Ramian, Schwettman and Smith, Physical Review Letters 38, 892-894 (April 18, 1977)
- 4) Elias et al., Physical Review Letters, 717-720 (March 29, 1976)
- 5) J. P. Reilly et al., "A Study to Design a Free Electron Laser Experiment, Volume 4", W. J. Schafer Associates, Inc. WSSA-FTR-79-135 (June 30, 1979)
- 6) Brau et al., "High Efficiency Free Electron Laser Systems," LASL Rept. LA-UR-79-3389 (Dec. 1979)
- 7) Elias, Luis R., Physical Review Letters 42, 977-981, (April 9, 1979)
- 8) Smith, Madey, et al., Journal of Applied Physics 50, 4580-4583 (July 1979)
- 9) Boeing Radiation Effects Laboratory/Mathematical Sciences Northwest, Free Electron Laser Experiment

## 4.0 LASER POWER RECEIVERS

### 4.1 INTRODUCTION

Several preliminary designs for power receiving stations were developed on the ground. Two types of receivers were considered, depending on assumed levels of ground level receiver intensities; namely,  $5 \text{ kW/m}^2$  (i.e., 5 times the normal solar intensity) and diffraction-limited intensities. In the latter case a 25 meter expansion telescope for the laser beam located in geosynchronous orbit will produce a 36 meter diameter spot size on the ground for 10.6 micron wavelength laser radiation in the diffraction limit. The telescope and receiver diameters each scale as the square root of the wavelength if both are allowed to change in size by the same amount. The limit to mirror optics is approximately  $20 \text{ W/cm}^2$  absorbed energy. Hence, for 1 percent absorption, this implies that the received intensities can be as high as  $2 \text{ kW/cm}^2$ . A 36 meter receiver could tolerate a total incident power of 20 GW, well above presently anticipated single unit power needs. Safety requirements may limit acceptable power levels to much closer to the  $5 \text{ kW/m}^2$  option.

### 4.2 PHOTOVOLTAICS

At lower power levels (e.g.,  $5 \text{ kW/m}^2$ ), a 1 GW incident power will require an area of  $2 \times 10^5 \text{ m}^2$  or a square approximately 450 meters on a side. The primary collector for this option can be photocells with additional Fresnel lens or reflective concentrators to increase the intensities focused onto each photocell. Since concentration ratios of 1000 appear feasible for photocells exposed to the total solar spectrum, we anticipate that similar intensities of laser radiation can also be used effectively. By choosing a semiconductor with a bandgap appropriate to the laser photon energy (e.g., gold doped Germanium for infrared laser radiation), relatively efficient energy conversion may be achieved. Because the infrared wavelengths best suited for high power gas lasers are similar to the background radiation characteristics (e.g., 8 to 10 microns), it may be necessary to cool the photocells. The power penalty for cooling should be minimal because thermal sinks existing on the earth such as rivers and the atmosphere can be used. The photocell conversion efficiencies should be limited only by diffusion and recombination kinetics within the semiconductor. Practical efficiencies as high as 40 to 50 percent may be achieved.

### 4.3 LASER-THERMAL POWER RECEIVERS

Alternatively, the  $5 \text{ kW/m}^2$  incident radiation can be collected by heliostats and focused on a power tower to drive a thermal power cycle. A central receiving cavity located at the heliostat focal point will be heated by the laser radiation and subsequently heat a high pressure working fluid which in turn can be used to drive a turbine generator. Solar power towers have been designed on this principle which use either helium, steam, or air as the working fluids, and promise to have overall cycle efficiencies of 18 to 20 percent (electric power incident solar energy). These efficiencies include losses due to reflection at the heliostats, incomplete coverage of the receiving area due to changing sun angle and shadowing, finite focal spot size due to the solar image size, as well as reradiation losses from the cavity and other thermal plant power losses. In contrast, laser radiation from a geostationary source can be focused through a very small receiver cavity aperture to make the reradiation and aperture cut-off losses negligible. Further, heliostat area coverage can be essentially 100 percent; some reflection losses will still be encountered, but these can be minimized by mirror coatings which are selective to the laser wavelength. Assuming similar thermal power plant efficiencies, the overall laser conversion efficiency should be closer to 40 percent compared to the solar power tower efficiency of 20 percent.

A previous study of laser driven heat engines indicated a potential for increasing the receiver conversion efficiencies further by using an inert gas working fluid such as helium doped with a small amount of a second gas (such as  $\text{SF}_6$ ) which resonantly absorbs the laser radiation. The absorbers transfer their energy very rapidly to the helium. Very high temperatures (up to  $3000^\circ\text{K}$ ) can be achieved leading to potentially high thermal efficiencies. Efficiencies on the order of 50 to 60 percent have been projected for laser driven heat engines. The technology would require completing the development of an efficient energy exchanger, a new power component device which currently is under development at MSNW. Typical receiver configurations for the photocell and power tower concepts are shown in Figures 4-1 through 4-3. Figure 4-4 shows some of the details of a typical laser driven heat engine.

SP-3284

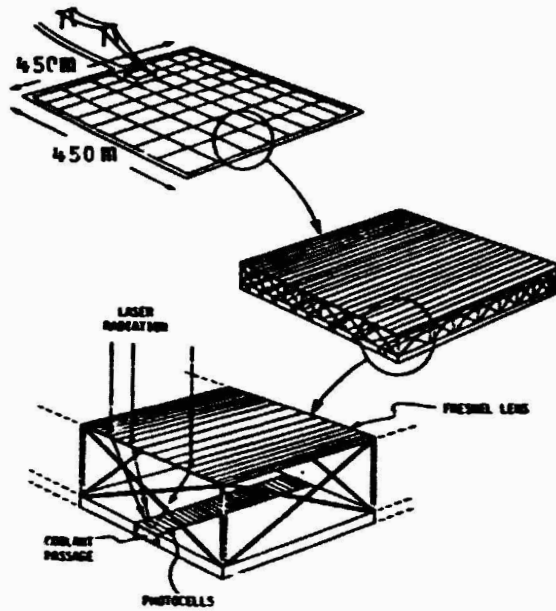


Figure 4-1: Photocell Receiver

SP-3285

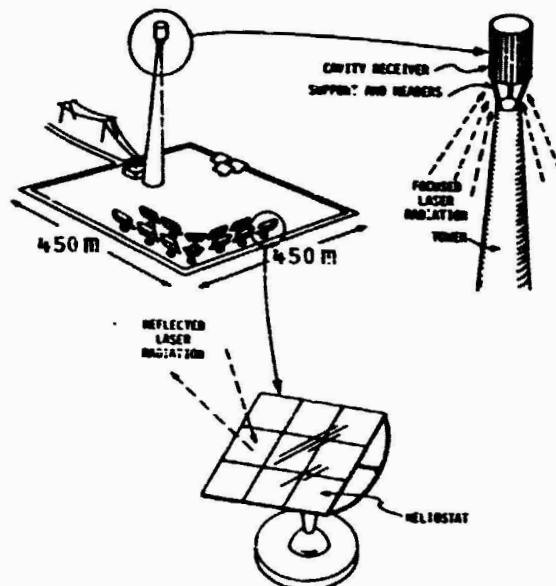


Figure 4-2: Power Tower Receiver

SPS 3204

ORIGINAL PAGE IS  
OF POOR QUALITY

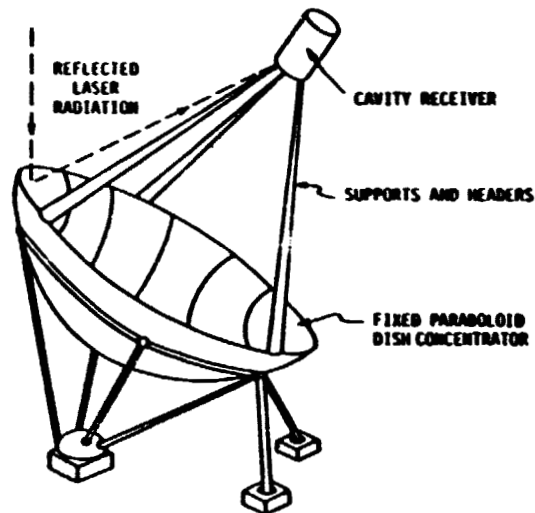


Figure 4-3: Single High Intensity Receiver

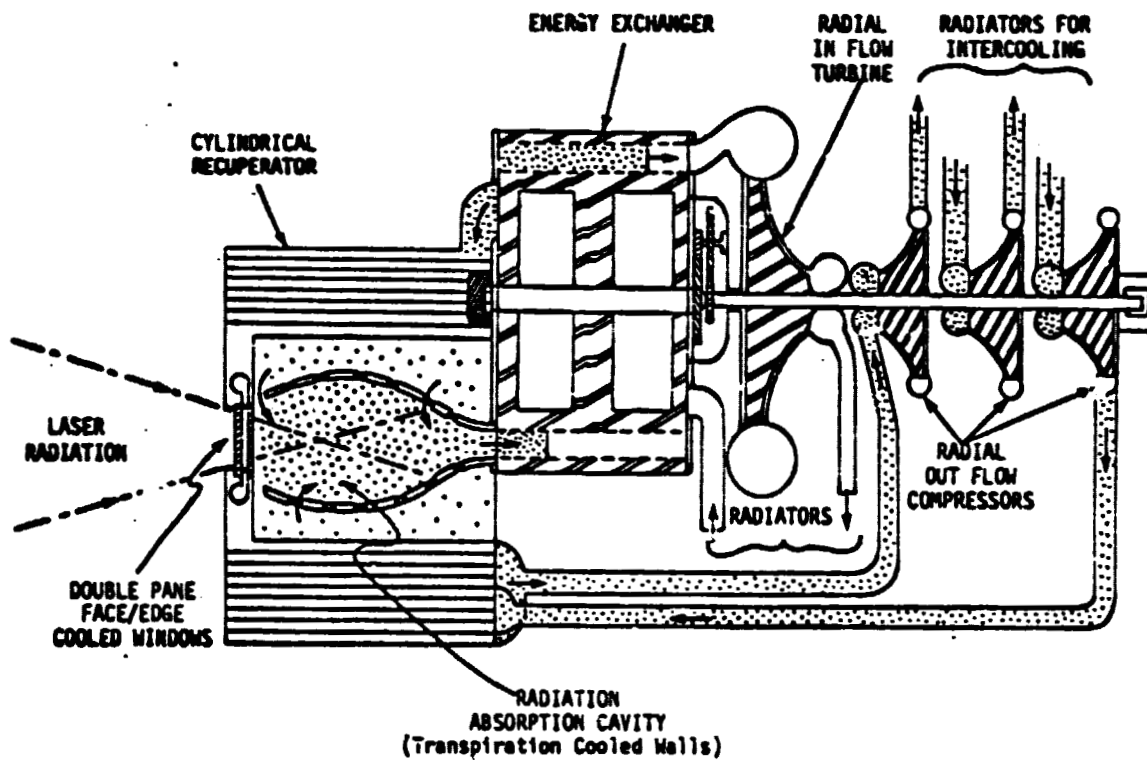


Figure 4-4: Schematic Cross Section View of Absorption Cavity, Energy Exchanger and Turbine of Laser Driven Heat Engine

#### 4.4 OPTICAL RECTENNAS

The optical rectenna consists of microminiature 10 micron wavelength dipole antenna and rectifier elements. It is entirely analogous to the microwave rectenna in principle of operation. (See Figure 4-5). Efficient optical rectenna operation requires incident laser intensities high enough (almost gigawatts/square meter!) to overcome forward voltage drops in the rectifying diodes. However, since a nominal factor of ten of concentration can be easily used and since all the laser concepts considered in this study can be pulsed (and all but the indirectly pumped laser must be pulsed) the desired peak fields can be achieved without exceeding average thermal limits.

The optical rectenna elements are fabricated on crystalline silicon sheets by standard semiconductor lithography and processing. The sheets, which should be made as large in area as possible, are mounted on plates at the base of a factor of 30 parabolic concentrator. Positive and negative power busses run along side for convenient power terminal connection. Under high average light intensities some water cooling of the rectenna sheets may be necessary.

Preliminary optical rectenna diode performance based on the constant forward voltage diode drop approximation is shown on Figure 4-6. Neither concentration or pulse factor alone will suffice for high efficiency - a concentration ratio of 30 to 100 with a pulse factor of 1000 to 10,000 is needed. The result is the most efficient laser receiver concept proposed to date.

If possible it is desirable to produce the optical rectenna sheets on a continuous production line much like that envisioned for SPS solar cells. Whether or not the statistics of random defects and impurities in the silicon sheets allows this has yet to be determined and is recommended as a subject for further investigation.

Another line of investigation that might prove useful for optical rectennas is the fabrication of antenna elements with gain so that the concentration and pulse factor requirements could be reduced. This might be done by using a slow wave structure in the plane of the rectenna panel, which could be canted at an angle to provide maximum antenna element gain. If a gain of only 20 db could be realized the optical concentrators could be eliminated, greatly simplifying the receiver configuration.

WFO-4287

ORIGINAL PAGE IS  
OF POOR QUALITY

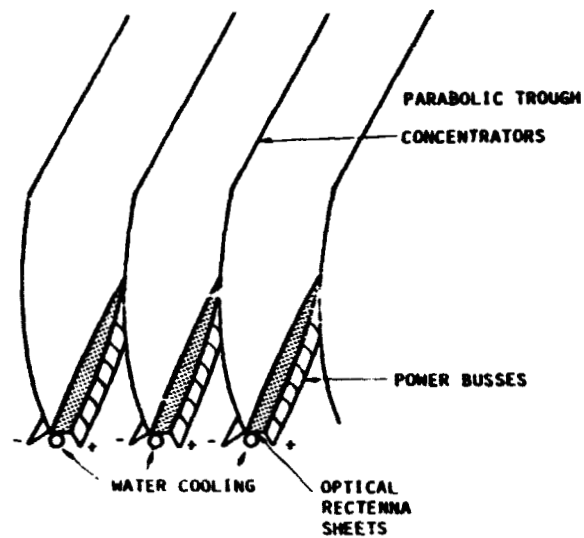


Figure 4-5: Optical Rectenna Configuration

WFO-4288

o DIODE OUTPUT VOLTAGE

$$V = \left( \frac{P}{A} Z_0 \right)^{1/2} \lambda$$

$\frac{P}{A}$  Power/Area     $Z_0$  Free Space Impedance     $\lambda$  Wavelength

o APPROXIMATE RECTENNA EFFICIENCY DUE TO FORWARD DIODE DROP LOSSES

$$\eta_{\text{forward}} = (V - V_{\text{forward}}) V^{-1}$$

for Silicon diodes  $V_{\text{forward}} = .6$  volts

o RESULTS OF CONCENTRATING ON DIODES AND PULSING LASER

CONCENTRATION	PULSE FACTOR	V (VOLTS)	$\eta_{\text{FORWARD}}$
1	1	.014	0
20	1000	1.94	.69
30	1000	2.38	.75
100	1000	4.34	.86
300	1000	7.52	.92
300	10000	23.8	.975

Figure 4-6: Optical Rectenna Preliminary Characteristics

#### 4.5 SUMMARY

Photovoltaics, thermal engines and optical rectenna diodes are candidates for the power receivers on earth in the laser SPS system design. While photovoltaic energy conversion of a laser beam will be more efficient than the conversion of sunlight, the basic physics of room temperature photovoltaics limits attainable efficiencies to around 40%. Cooling the receptors improves this but requires unattractive refrigeration powers. Thermal engine power receivers much like the solar power tower installations now being constructed in the southwest are expected to have reception efficiencies around 60%. In fact, the existing solar power towers could probably be used by just repointing the already steerable reflectors. Finally, one might take advantage of modern electronic lithography to fabricate optical receiving dipole/diode elements directly analogous to microwave rectenna elements. Light-to-electric efficiencies exceeding 80% may be attainable.

PRECEDING PAGE ELEMENT NOT FILMED



## 5 - INDIRECT OPTICALLY PUMPED LASER SPS CONSTRUCTION

The construction methods used to assemble the 100 MW Indirect Optically Pumped Laser Solar Power Satellite (IOP Laser SPS) are similar to those previously described for assembling the 5000 MW reference photovoltaic SPS (D180-25461-3) and the earlier SPS concepts which used thermal engines (D180-20689-3 and D180-22876-3/-5). This laser power satellite is assumed to be fully assembled in GEO in accordance with the reference scenario. Hence the GEO construction base and its operations were structured to meet the peculiar requirements of the IOP Laser SPS design. Wherever possible, the reference system groundrules and constraints have been followed. For example, the reference SPS Construction Base, which is shown in Figure 5-1, is required to assemble one 5 GW reference satellite every six months, or produce 10 GW system capacity each year for 30 years. As discussed below, this annual production goal cannot be achieved with a single laser SPS construction base. Other major groundrules and constraints for the operation of GEO base systems, are shown in Figure 5-2. The base is required to provide contiguous facilities for assembling all satellite system elements so as to avoid free-flying construction facilities and/or assembly methods. As a GEO operational base, the Laser SPS Construction facility is also required to support the maintenance and repair of operational SPS systems. Therefore, the GEO base must be capable of docking and unloading orbital transport vehicles; and implementing other essential work support and crew support functions as defined for the reference system (D180-25461-2). GEO base operation timelines in turn, are based upon two 10 hour shifts/day and rely upon IVA operations only, except for emergency EVA. These requirements are extracted from the Phase 2 study reports (D180-25461-3/4) and guide the definition of all other requirements.

The GEO base for constructing the 100 MW IOP Laser SPS is shown in Figure 5-3. This laser construction base is significantly smaller than the reference GEO base for building the 5000 MW photovoltaic SPS concept. The largest construction job associated with the IOP Laser SPS system is to build the concentrator and the facility, for this activity dominates the base, as shown in Figure 5-3. Building the laser transmission system is essentially an assembly operation and the facility for this activity is mounted to the spine of the concentrator platform. The laser construction base is discussed more fully below.

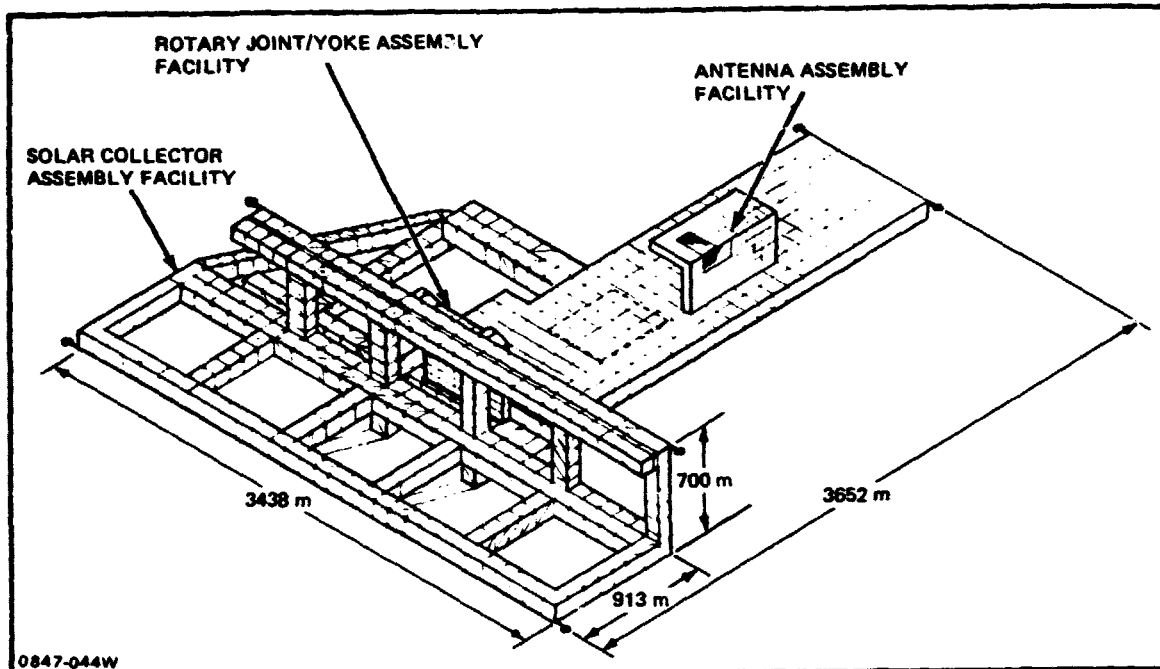


Figure 5-1 4 Bay End Builder – Reference SPS Construction Base

- CONSTRUCT ONE 5 GW SPS WITHIN 6 MONTHS  $\pm 5\%$  (OR PRODUCE 10 GW CAPACITY/YEAR)
- USE CONTIGUOUS FACILITIES TO ASSEMBLE SATELLITE ELEMENTS
- SUPPORT MAINTENANCE OF OPERATIONAL SPS SYSTEMS
- DOCK, OFFLOAD & SERVICE POTV, CARGO TUG & OTV
- PROVIDE ESSENTIAL WORK FACILITIES & CREW SUPPORT FACILITIES
- TWO 10 HR SHIFTS/DAY @ 75% EFFICIENCY, 6 DAYS/WEEK
- BASELINE IVA OPERATIONS – EVA EMERGENCY LIMITED

0847-045W

Figure 5-2 GEO Construction – Major Groundrules and Constraints

CONSTRUCTION IS  
OF POOR QUALITY

Figure 5-4 presents a top level comparison of the IOP Laser Construction Base with the baseline GEO Construction Base. It shows the GEO base for IOP Laser SPS construction to be considerably lighter (due to its small size), than the Phase 2 reference base. However, this base requires a much larger crew for construction operations and yet it only provides 2% of the annual production goal (0.2 GW vs 10 GW). As a result of the larger crew, the unit cost and annual cost of the IOP Laser Construction Base are 30% higher than the Phase 2 reference.

It should be noted that the Solid State SPS Construction Base described in Volume 4 also falls short of the 10 GW/yr production goal, but is only 15% less. The 2500 MW Solid State SPS concept has an antenna double the size of the reference concept which is on the critical path for construction. Although the IOP Laser SPS has a different solar conversion system, its solar concentrator is of a comparable structure and size to the solid state SPS antenna. It would be reasonable to conclude that if the solid state SPS construction base can produce nearly four antennas per year, then a similar construction base could produce a like number of solar concentrators for the laser SPS. Unfortunately, a laser SPS with this size concentrator can only be produced at the rate of two per year which yields 0.2 GW annual capacity. Thus, a 10 GW/yr production rate for a single laser SPS construction base seems unlikely.

The rationale for the low annual productivity due to the IOP Laser SPS concept is discussed further below. The following paragraphs describe the analysis performed of laser satellite construction and the features required for the GEO construction base.

## 5.1 CONSTRUCTION OPERATIONS REQUIREMENTS

The 100 MW Indirect Optically Pumped Laser (IOPL) Solar Power Satellite (SPS) is to be constructed entirely in GEO and is to be assembled in accordance with the major groundrules and constraints for the reference construction base wherever possible. That is, to use contiguous assembly facilities, operate two 10-hour/shifts/day at 75% efficiency, etc, appears reasonable. The 10 GW annual production goal however, may be inappropriate for the 100 MW power category. The IOPL SPS features an off-axis parabolic concentrator with a black body cavity, radiator, and eight laser reflectors, as defined by recent Boeing data, (see Fig. 5-5). The solar concentrator is designed with a tetrahedral structure and is assumed to be covered with adjustable reflective facets, similar to those used on earlier solar thermal SPS concepts (Refer to Report D180-20689-3).

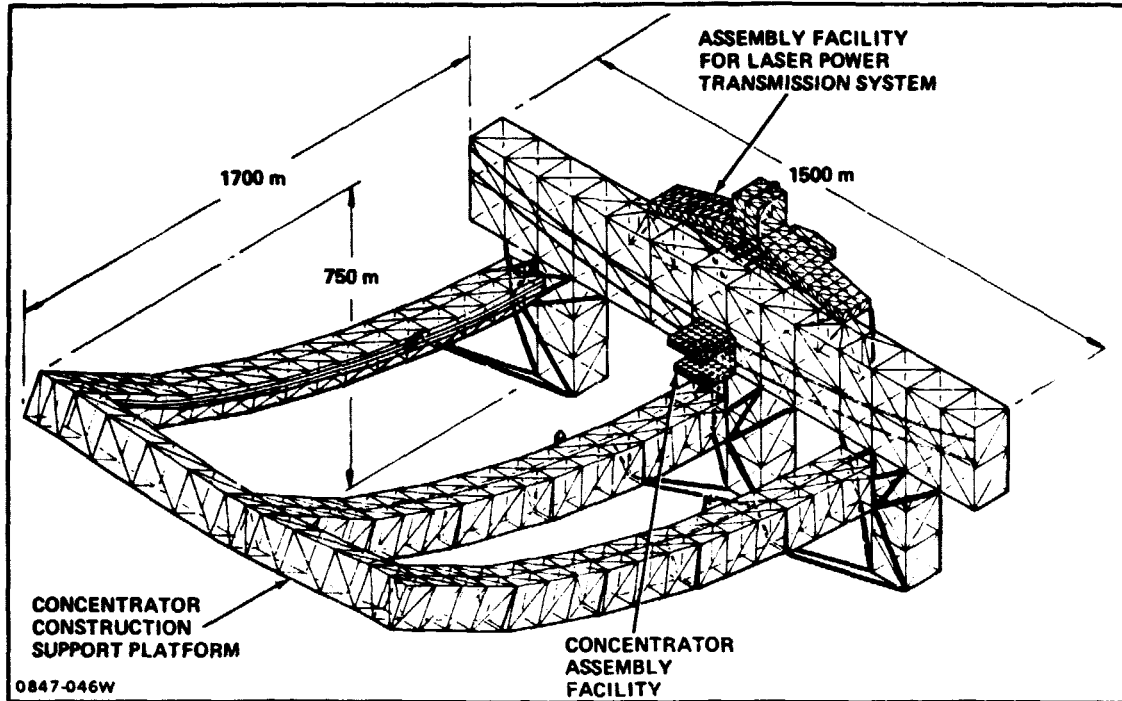


Figure 5-3 Indirect Optically Pumped Laser SPS Construction Base

ORIGINAL PAGE IS  
OF POOR QUALITY

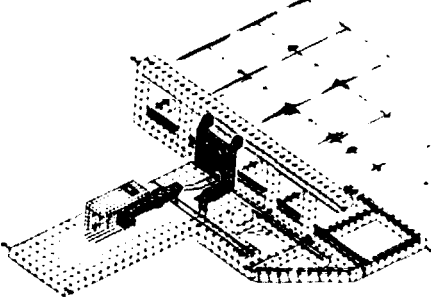
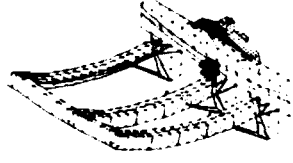
	BASELINE	IOP LASER
		
<ul style="list-style-type: none"> <li>• SPS PRODUCTION RATE</li> <li>• BASE UNIT COST, 1979\$</li> <li>• BASE ANNUAL COST</li> <li>• BASE MASS</li> <li>• CONSTRUCTION CREW</li> </ul>	<p>10 GW/YR \$ 9.01B \$ 1.30B/YR 6656 MT 444</p>	<p>0.2 GW/YR \$ 12.09B \$ 1.71B/YR 4950 MT 587</p>

Figure 5-4 SPS Construction Base Comparison – Baseline vs IOP Laser

As in the reference SPS, a broad range of technology issues (most of which are beyond the scope of this study) must be addressed to cover all aspects of the laser SPS construction process. These are listed in Figure 5-5. If this concept is to be studied further, the satellite construction approach must be reexamined for the solar concentrator, laser power transmission, and interface systems. In addition, the structural assembly methods should be well understood to the level of beam fabrication, handling and joining. Techniques for assembling and installing the major subsystems (i.e., facets, lasers, buses, reflectors and radiators) must be further developed and the requirements for construction equipments need further refinement. In addition, the structural dynamic, thermodynamic and control interactions between the base and the satellite should be investigated and defined. Other areas to be examined include methods for berthing or mating of large system elements, techniques for in-space inspection and repair, and concepts for implementing satellite final test and checkout.

#### 5.1.1 Satellite Construction Timeline & Analysis

A timeline for constructing the IOPL-SPS is shown in Figure 5-6. As in the reference system, it features parallel assembly of the solar concentrator system and the laser power transmission system. The interface system is constructed as needed for final systems mating. The times for interface assembly, systems mating, and final test and checkout are assumed to be the same as for the reference system. However, the longer time shown for assembling the two major systems was determined from analysis of concentrator assembly operations.

Overall operations analysis for construction of the IOPL-SPS is shown in Figure 5-7. It follows the same sequence as the reference 5 GW Microwave SPS. The construction operations for the solar concentrator system received the major emphasis and were analyzed from the top down. A breakdown of the assembly operations for the Laser SPS Solar Concentrator system is shown by the abbreviated flow illustrated on the lower half of the figure. This assembly activity includes the fabrication and assembly for the first row of primary structure (function 3.1.1). It also includes the parallel installation and inspection of other subsystems during the construction process. These subsystems include the installation of facets (function 3.1.2) attitude control, etc. When each row is assembled, the concentrator is indexed (function 3.1.6) away to allow the second row to be added. The remaining rows of the concentrator are constructed in a like manner.

ORIGINAL PAGE IS  
OF POOR QUALITY

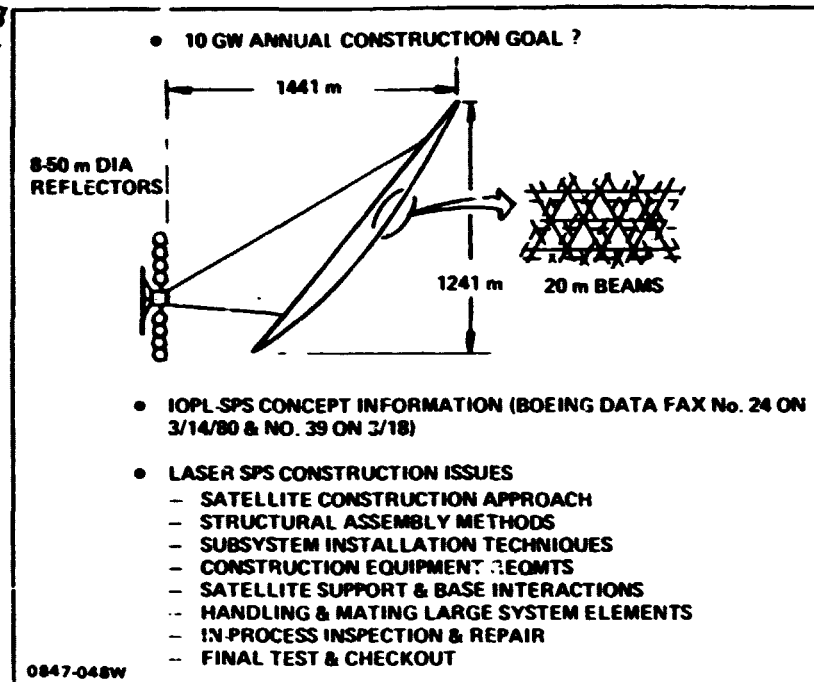


Figure 5-5 Indirect Optically Pumped Laser SPS Construction Requirements & Issues

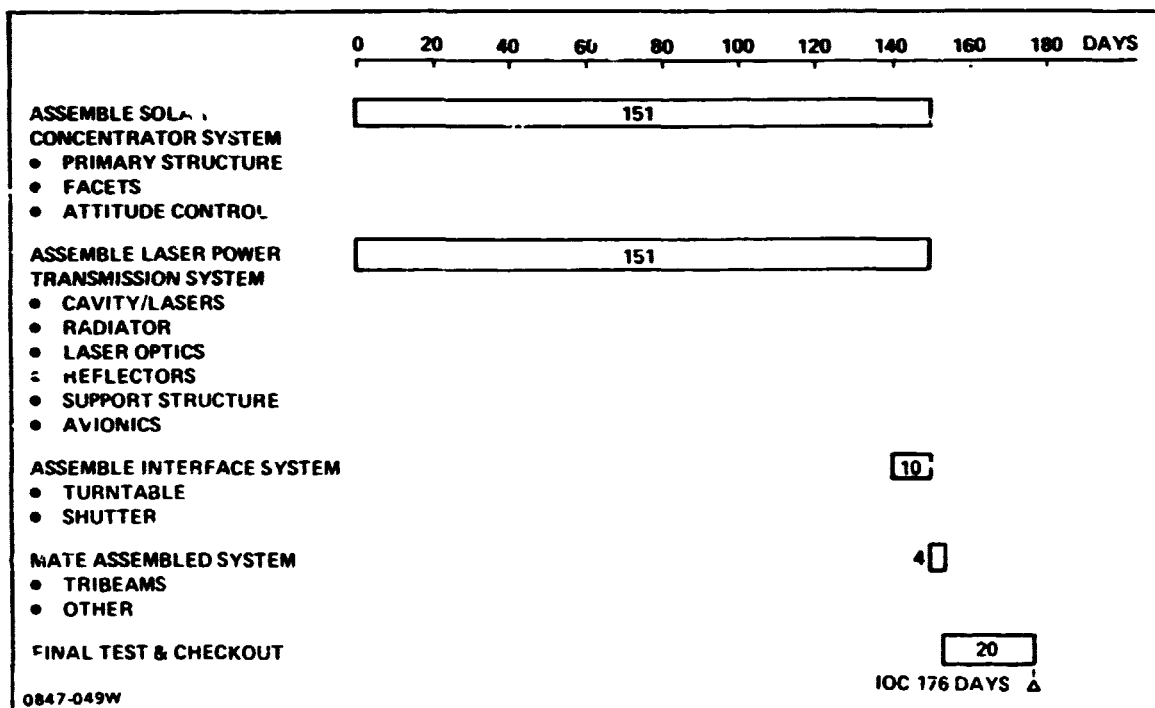


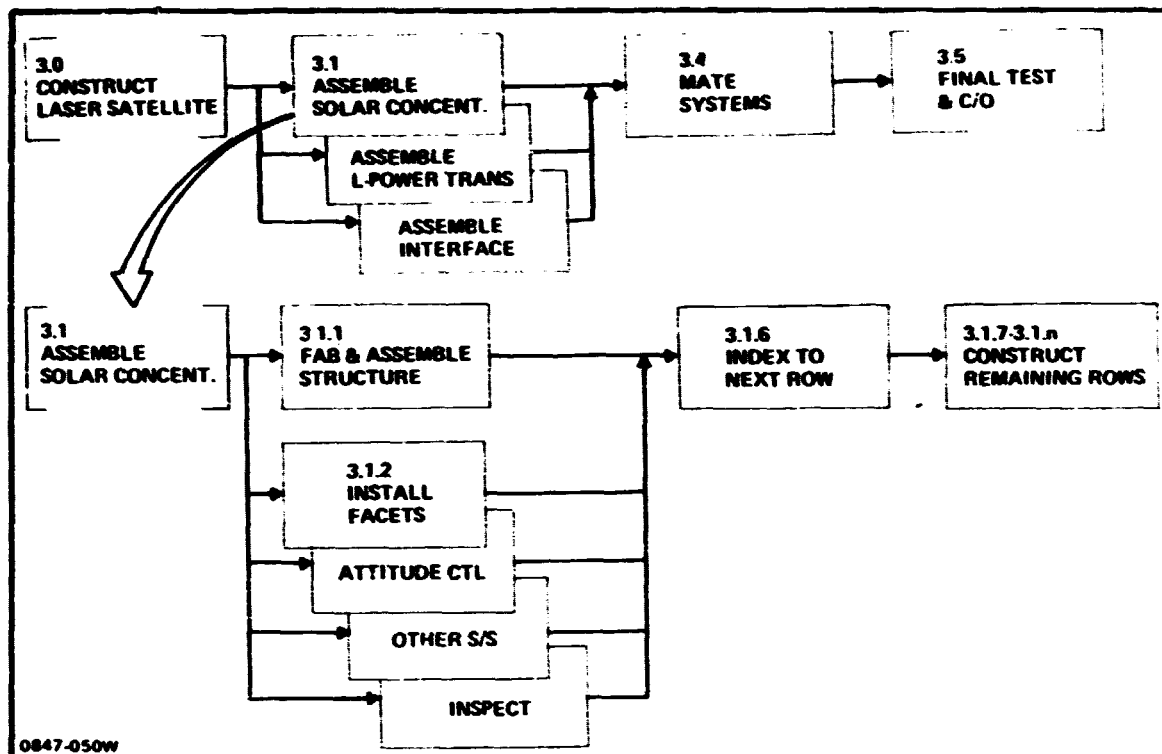
Figure 5-6 Indirect Optically Pumped Laser SPS Construction Timeline







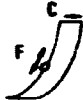

### 5.1.2 Concentrator Construction Requirements

Shape of the concentrator is a big factor in the ease of its construction. Figure 5-8 considers some alternate means of providing the concentrator surface paraboloid shape with non-parabolic structures. To build an offset paraboloid shaped structure with maximum repeatability requires a facility indexing along a parabolic curved track, building as it goes a row of varying geometry structural bays assembled from beams of varying lengths. At completion of a row, the structure is indexed outboard, ready for assembly of the next row. Each row is repeatable but owing to the variation in beam lengths, as much as 50% above or below the 20 m nominal, the assembly facility must be large enough to handle beams up to 30 m long. Indexing the paraboloid shape structure as it is built, requires curved support arms, each of which is a different radius from another. Steerable facets, which provide the reflective surface, are mounted to primary structure node points but, due to the varying geometry of structural units, the nodes do not provide a regular pattern. Therefore, to minimize concentrator surface, the facets must vary in size to match the node pattern. An alternate is to provide a secondary structure which provides regular pattern mounting points for constant size facets. Concentrator area is the minimum necessary.

Since steerable facets will be used in any event to provide the parabolic reflective surface, then a more simply built structure on which to mount them can be considered. A segment of a sphere which approximates the paraboloid segment can be built by a facility indexing along a circular track to follow the same construction procedure as the paraboloid. Here, however, support arms for the indexing concentrator have the same radius. Variation in primary structure beam length is  $\pm 10\%$ , much less than the parabolic structure. The structure bay varies progressively in geometry over half of one row then reverses the variation over the remainder of the row. This total variation is repeated for each row. Spherical concentrator structure area must be about 10% larger than a tailored parabolic area since the facets must be spaced to reflect into the paraboloid focus, as shown on the following chart. To keep this area increase to a minimum requires, again, either a secondary structure on which to mount constant size facets or no secondary structure but facets varying in size to suit primary structure geometry. An alternate is to use constant size facets but increase the concentrator area to provide the necessary facet mounting points. The construction timeline is affected by the size as well as the variation in structure unit geometry.

Simplifying the construction base even further leads to the other two structural shape options shown on the chart, a parabolic trough and a flat surface. These require up to 40% larger concentrator areas with little reduction in base complexity.



	PARABOLOID SEGMENT		SPHERE SEGMENT			PARABOLIC TROUGH			FLAT		
• CONCENTRATOR STRUCTURE SHAPE											
• CONCENTRATOR INDEXING (F = FACILITY C = CONCENTRATOR)											
• CONCENTRATOR SUPPORT	MULTI-CURVE		SINGLE-CURVE			STRAIGHT			STRAIGHT		
• PRIMARY STRUCTURE - BEAM LENGTH VARIATION (20 m NOMINAL)	~ ± 50%		~ ± 10%			~ ± 10%			NONE		
• SEPARATE FACET SIZE	SAME	VARIED	SAME	SAME	VARIED	SAME	SAME	VARIED	SAME	SAME	VARIED
• SECONDARY STRUCTURE	YES	NO	YES	NO	NO	YES	NO	NO	YES	NO	NO
• CONCENTRATOR AREA INCREASE	NORM	NORM	<10%	10%	<10%	<20%	20%	<20%	<40%	40%	<40%

IF FACETS RECD  
MINIMAL IMPACT  
ON ASSEMBLY FACILITY  
& CONCENTRATOR  
AREA

0847-051W



One other option is to dispense with the separately mounted, steerable facets and mount reflective sheet directly to the primary structure. This greatly increases the accuracy with which the structure must be built and dictates that it be a segment of a paraboloid of revolution, a much more complex construction operation. This option requires further study. The selected option is the spherical segment concentrator which uses constant size facets but no secondary structure. Its small area penalty has little impact on production.

Having selected separate steerable facets mounted on a spherical segment to provide a paraboloid surface, Figure 5-9 shows the paraboloid shape (dotted lines) superimposed on a comparable spherical surface (solid lines). In a section through the principal axis of the paraboloid, the surfaces are fairly close in form but in a section normal to the principal axis, they diverge quite a bit either side of a common center-line. This divergence in surfaces requires that the spherical surface be large enough to mount the facets at a spacing which provides unrestricted reflective paths to the parabola focus. The area of the spherical surface is, therefore, larger than the corresponding parabolic surface. The additional area is, of course, a function of the geometries.

Concentrator Assembly Method - The sequence for building the concentrator is shown in Figure 5-10. It is an assembly of repeatable rows of structural bays. The facility indexes across the construction base via a track system to fabricate and assemble the first row as it goes. The completed row, supported by two holding fixtures mounted to a track on the construction base, is then indexed forward for one row width. The facility is then indexed back along the track building the second row onto the first row, during this second construction pass. This process is repeated until the concentrator is completed. Taking a more detailed look at the sequence as it builds the first rows, the facility starts by building primary structure for the first four bays of the first row. The facility then indexes four bay lengths, then builds the structure for the next four bays. This is repeated until the first row is completed. The first row is then indexed forward one row. The facility then builds four bays of the second row on to the first row, it is then indexed back four bay lengths to build that structure. The process is repeated, with each completed row indexed forward on the construction base and the facility building as it is indexed from side to side, until the start of the third row. With the start of the third row, the reflecting facets, which have been assembled in the high bay area of the facility, are installed on the completed rows of the concentrator. Two of the hexagon shaped facets are installed for

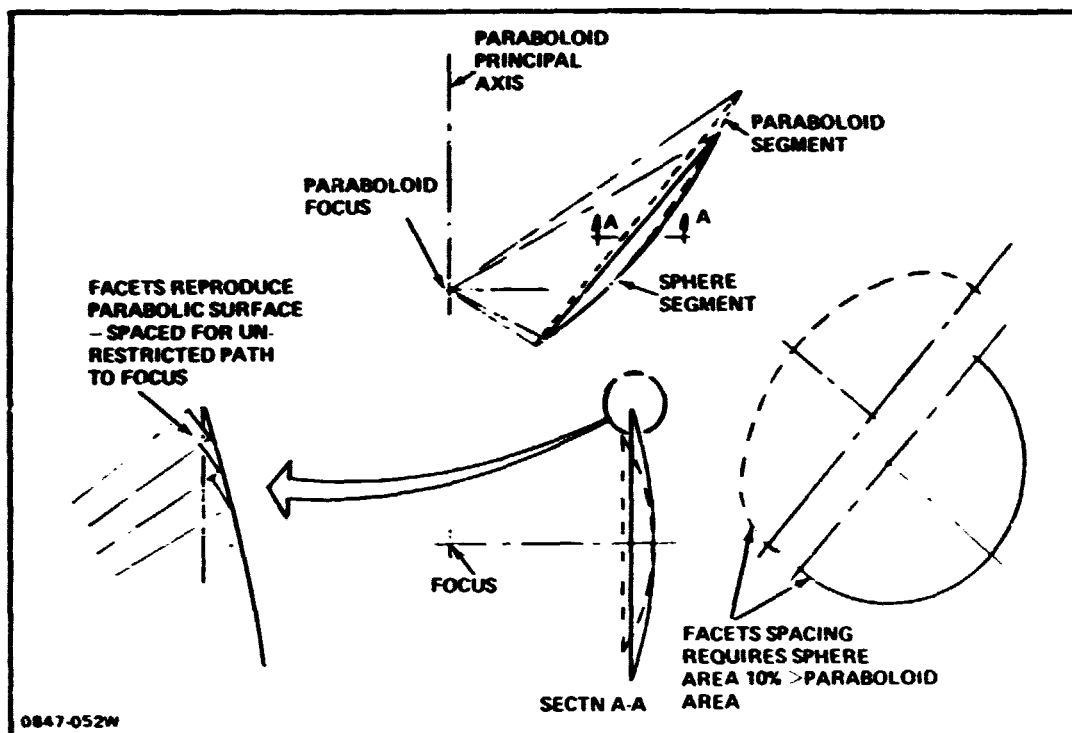


Figure 5-9 Parabolic Concentrator Surface Mounted on Spherical Segment

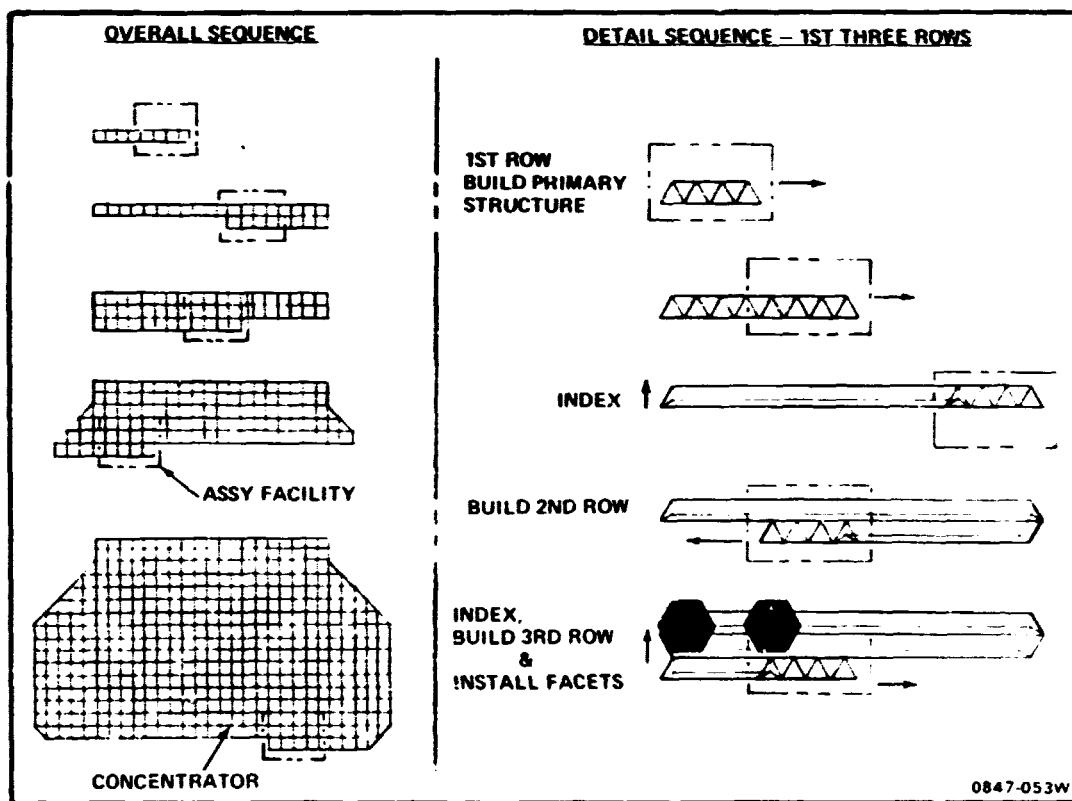


Figure 5-10 Concentrator Construction Sequence

each of the following four structural bays. This process is repeated until the concentrator structure is completed and approximately 1500 facets installed.

Figure 5-11 shows a timeline for building the first three rows. There are 44 tetrahedral bays in the first row of construction, which are built four at a time. The entire concentrator has 4656 tetrahedral bays. By building 4 bays at a time, fabricating 2 beams with each beam builder at 1.5 mpm, and considering related operations (e.g., setup, joining, indexing, etc) this completed structure is estimated to take 148 days. Sequential installation of the reflective facets and other subsystems parallels the assembly of the third structural row near the start of day 3, as shown. Hence, the total assembly time is 151 days.

Concentrator Assembly Operations - As described above, four build stations are required in the assembly facility, for the fabrication and assembly of the concentrator primary structure. The concentrator consists of approximately 42,000 (1.5 m x 20 m (nominal)) beams assembled to form the tetrahedral structure of the spherical concentrator. Figure 5-12 identifies the equipment needed for the fabrication and assembly of the structure at one of the four build stations. As shown, each beam machine fabricates two of the 1.5 m x 20 m beams required and the cherry pickers are used for the alignment and assembly of the beams. Eighteen 1.5 m beam machines, twenty-nine 30 m cherry pickers and four 10 m indexers are required to support the four build stations to fabricate and assemble four structural bays of the concentrator.

Another area required in the assembly facility is the facet assembly station shown in Figure 5-13. To provide the parabolic reflecting surface requires approximately 1500 facets mounted to the primary structure. For each facet, operations at the assembly stations consist of assembling the three radial support arms, edge members, tension bridles and the pre-cut reflecting film. The completed facet assembly is then attached to a central mounting post which has been attached to the tetrahedron structure of the concentrator.

### 5.1.3 Other Construction Requirements

Turning to the laser power transmission system, as presently configured, it has eight reflectors transmitting to the ground. Figure 5-14 shows the main subassemblies of a reflector and identifies gross assembly operations for building the reflectors from ground-fabricated components. The primary mirror is 50 m in diameter and is an assembly of segments, each of which has a primary structure, supporting adaptive optics. A secondary mirror is supported from the primary mirror by struts.

ORIGINAL PAGE IS  
OF POOR QUALITY

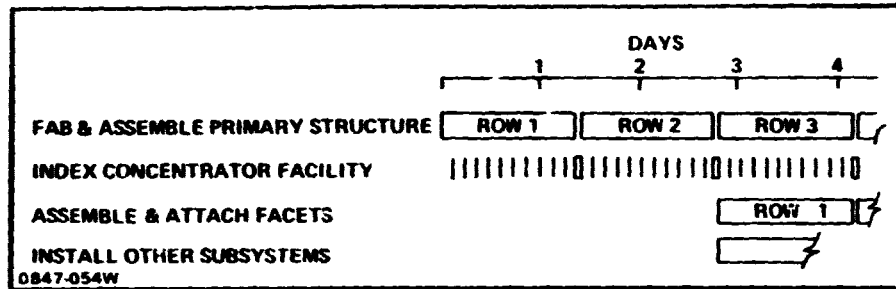


Figure 5-11 Concentrator Assembly Timeline

### CONCENTRATOR STRUCTURE FABRICATION & ASSEMBLY

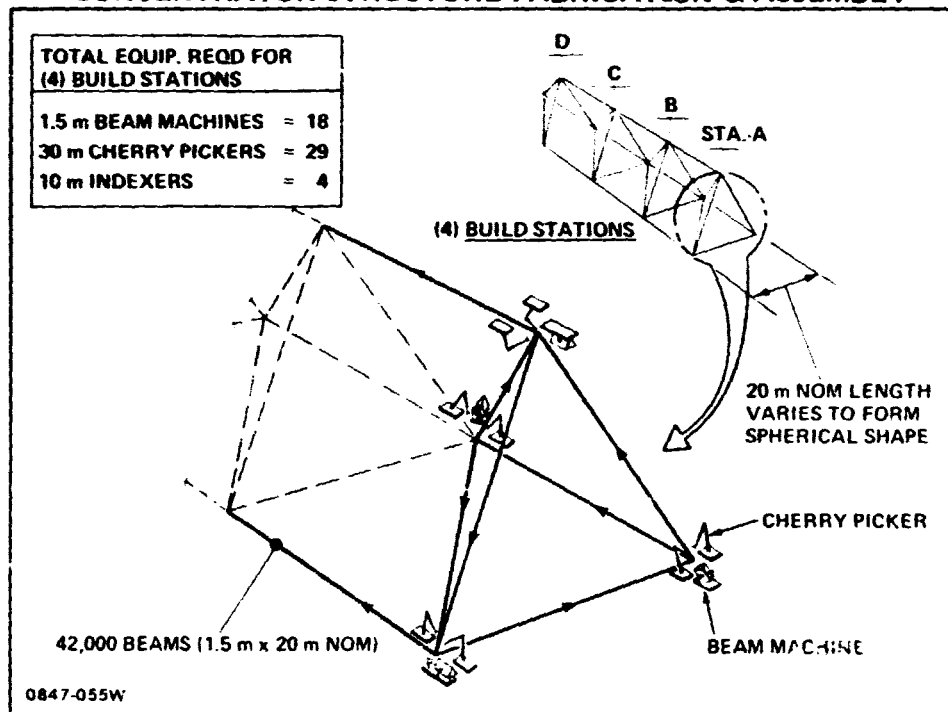


Figure 5-12 Concentrator Structure Fabrication & Assembly

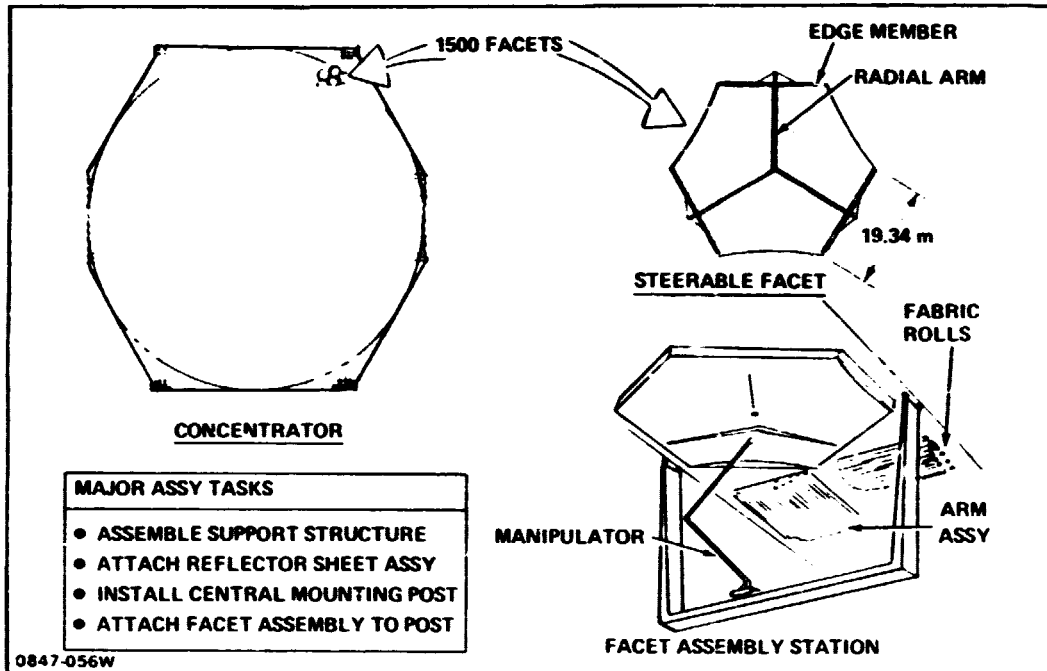


Figure 5-13 Concentrator Facet Installation Requirements

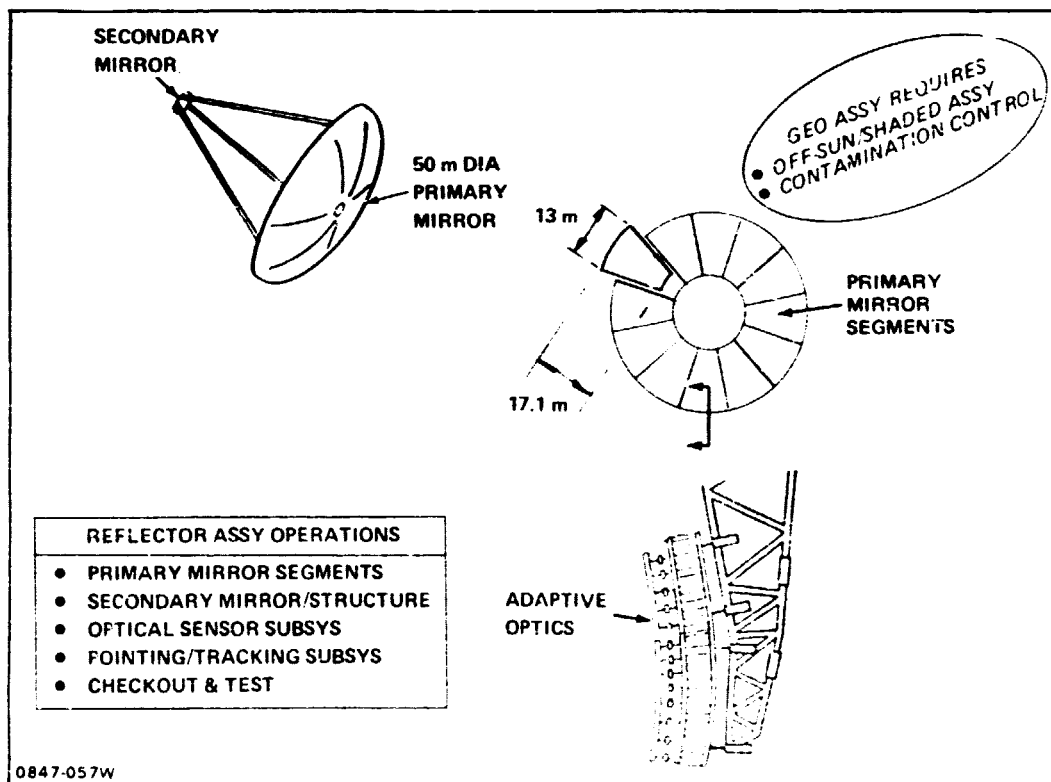


Figure 5-14 Laser Reflector Assembly Requirements

Assembly should be done out of the sun and, to this end, a shading facility is provided on the construction base. Contamination control during assembly is necessary to ensure satisfactory operational performance.

The other main component of the laser power transmission system is the laser cavity assembly which has a cavity wall lined with pyrolytic material, assembled from segments. Figure 5-15 shows that eight laser units are mounted around the cavity opening. Each laser unit (about 10 m high x 10 m wide x 5 m deep) contains numerous 10 m-long laser transparent tubes (i.e., glass) which are exposed to the black body cavity. These preassembled units will require special handling and each of the other elements will have other peculiar requirements to contend with. For example, a large radiator, which cools the lasers, is mounted to the cavity unit by support struts. Gross assembly operations are listed for building the cavity and its appendages from ground-fabricated subassemblies.

In considering the complexity of laser power satellite assembly operations, Figure 5-16, lists the gross elements comprising a satellite and identifies the assembly functions necessary for each. The functions are classified as structural, mechanical, electrical, fluid and optics. All elements require structure assembly and, with the exception of basic structural subassemblies, they all require electrical assembly. Many mechanisms are involved in these elements, and each must be assembled and installed. Fluids are expected to be in self-contained subunits which need no open fluid connections. Optical assemblies will require alignment by adjustment as they are assembled, or during checkout. These operations are diverse, and in some cases, require dedicated equipment which have yet to be defined.

## 5.2 LASER SPS CONSTRUCTION BASE

The GEO construction base for the IOP Laser SPS concept is shown in Figure 5-17. This base, which is comprised of open truss members (see Fig. 5-3), is 1.5 km wide x 1.7 km long x 0.75 km deep, whereas the reference base is much larger (i.e., 3.44 km wide x 3.65 km long). The laser construction base has contiguous facilities for concurrent assembly and subsequent mating of the solar concentrator and laser power transmission systems. This base supports the satellite during all phases of construction. For example, a curved assembly platform is provided to support the construction of the spherical solar concentrator. This spherical shaped structure, in turn, is assembled by a small facility which moves across the base along a curved track. The concentrator is built one row at a time which is similar to the method of assembly described for the SPS solid state microwave antenna (Report D180-25969-4). The

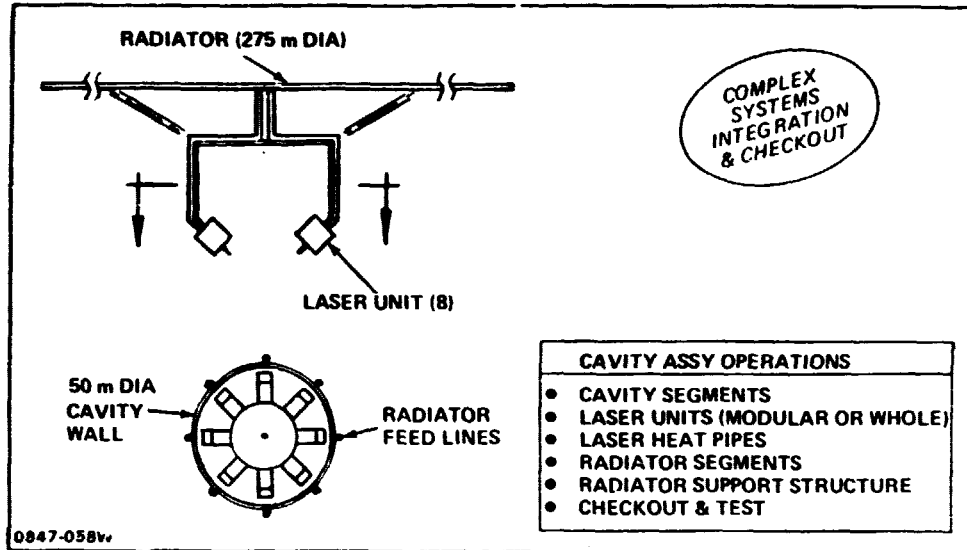


**Figure 5-15 Laser Cavity Assembly Requirements**

IOP LASER SPS ELEMENTS	FUNCTIONS				
	STRUCTURAL	MECHANICAL	ELECTRICAL	FLUID	OPTICAL
<ul style="list-style-type: none"> <li>• SOLAR CONCENTRATOR               <ul style="list-style-type: none"> <li>- PRIMARY STRUCTURE</li> <li>- FACETS</li> <li>- ATTITUDE CONTROL</li> </ul> </li> </ul>	• • •	• •	• •	TANKS	•
<ul style="list-style-type: none"> <li>• LASER POWER TRANSMISSION               <ul style="list-style-type: none"> <li>- CAVITY</li> <li>- LASER UNITS</li> <li>- SUPPORT STRUCTURE</li> <li>- RADIATORS</li> <li>- LASER OPTICS</li> <li>- LASER REFLECTORS</li> <li>- ELECTRICAL POWER</li> <li>- AVIONICS</li> </ul> </li> </ul>	• • • • • • • •	• • • •	• • • • • • • •	SEALED  SEALED	•   • •
<ul style="list-style-type: none"> <li>• INTERFACE               <ul style="list-style-type: none"> <li>- TURNTABLE</li> <li>- SHUTTER</li> <li>- TRIBEAMS</li> </ul> </li> </ul>	• • •	• •	• •		

DIVERSE ASSEMBLY OPERATIONS TO BE PERFORMED

0847-059W

**Figure 5-16 IOP Laser Power Satellite Assembly Functions**

OF POOR QUALITY

concentrator assembly facility can progressively build a spherical tetrahedral structure and install steerable facets as it goes in either direction. Simultaneously, the laser power transmission system is assembled in a separate facility which is mounted to the base of the concentrator assembly platform. Here, the laser cavity, radiator, turntable, shutter assembly and the 50 m diameter reflectors with their support structures, are assembled. For final assembly, the laser power transmission assembly is located in its correct operational position, relative to the concentrator, by an arm pivoted from the base. Struts to join the concentrator to the transmission assembly are then fabricated and installed.

#### 5.2.1 Concentrator Assembly Facility

The concentrator assembly facility is shown in some detail in Figure 5-18. The "C" shaped mobile facility, 94 m high x 100 m wide x 100 m long, is shown mounted to the construction base via a track system which allows the facility to index from side to side to build the rows of structural bays of the spherical shaped concentrator. This facility covers four bays of the concentrator structure and builds in two directions. The inboard low bay area of the facility provides four stations for building the concentrator structure. Located at these stations are 1.5 m beam machines for the fabrication of the structural beams and 30 m cherry pickers for the alignment and assembly of the beams. In parallel with the building of the structure, the concentrator reflecting facets are assembled in the facet assembly station located in the outboard upper high bay of the facility. Facet assemblies are then installed on the completed structural bays.

An overall construction sequence to be followed, when building a laser SPS, was described in Subsection 5.1.2. When the two major assemblies of the satellite have been built (i.e., concentrator and the laser power transmission), they are located in their separate facilities, ready for final assembly (see Fig. 5-19). The concentrator assembly facility is shown tracking back to its stowed location.

#### 5.2.2 Final System Mating Arrangement

Final mating of the satellite systems is shown in Figure 5-20. Before mating the laser power transmission system to the concentrator, it must first be located in its operational position. This is accomplished by a support arm, part of the construction system, which first attaches to the transmission unit at its shutter assembly mounts, then pivots to position it at the operational location. A small platform, mounting a 7.5 m beam, is located at the tip of the support arm where it attaches to the transmission. With the beam machine aimed at one of the four interface beam attachment points on



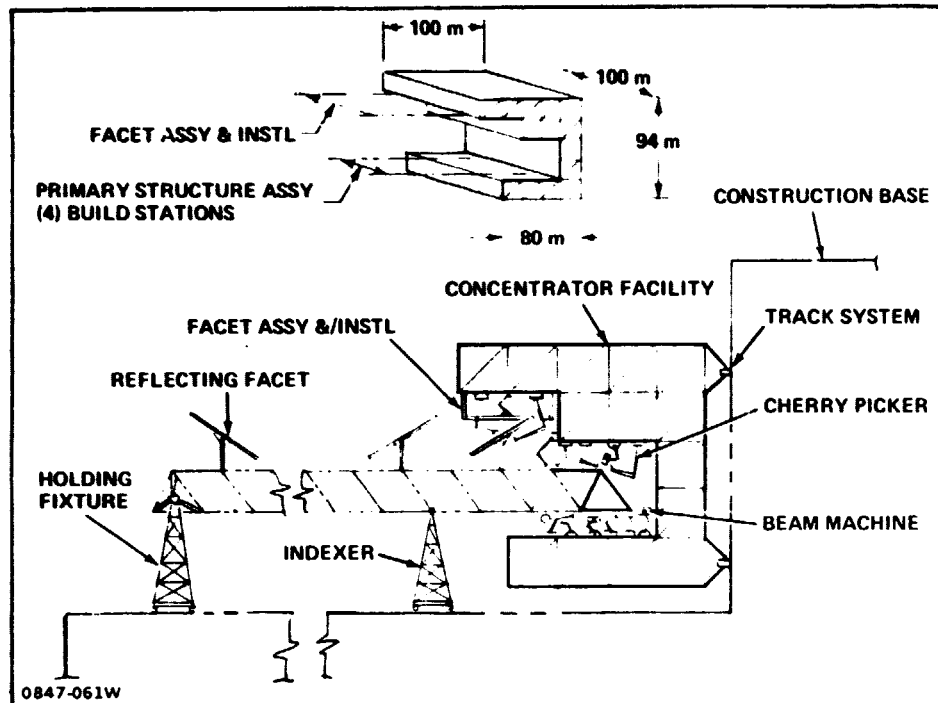


Figure 5-18 Concentrator Assembly Facility

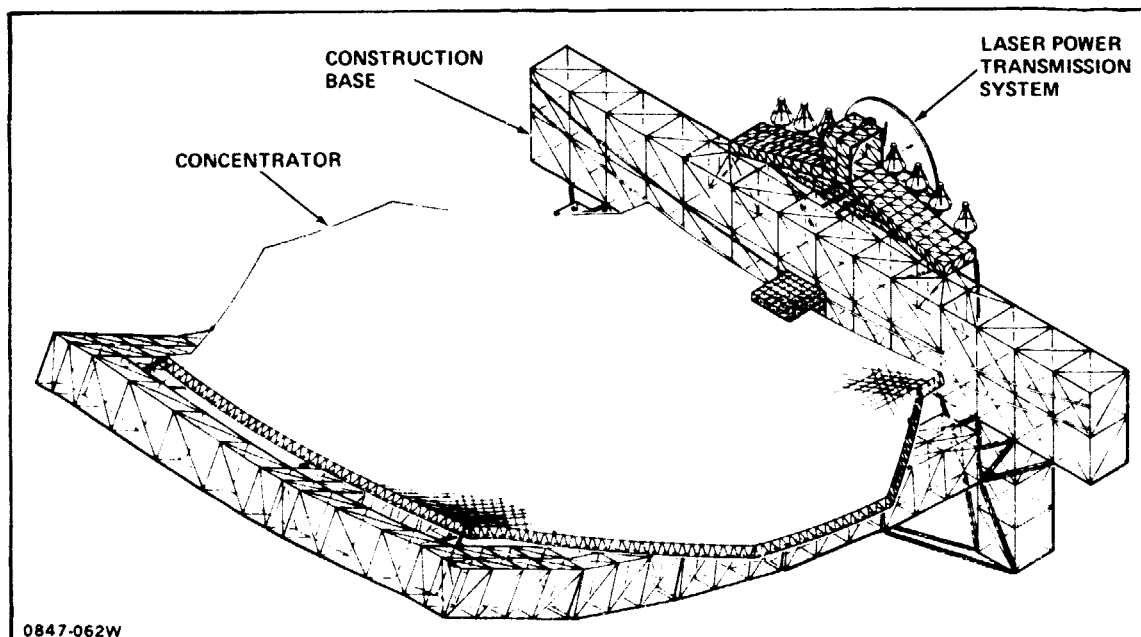


Figure 5-19 Laser SPS - Construction Completed

ORIGINAL PAGE IS  
OF POOR QUALITY

the concentrator, a beam is fabricated to arrive at this attachment point where it is mated to the concentrator. The other end of the beam attaches to the transmission assembly at the shutter mount. This process of beam machine alignment, beam fabrication, and installation is repeated for the three other interface beams.

### 5.2.3 Construction Equipment & Crew Operations

Figure 5-21 lists the construction equipment, identified to date, for building the IOP Laser SPS concept. A breakdown of equipment used to assemble the solar concentrator is shown, together with related mass and cost estimates. The large number of 1.5 m beam builders and 30 m cherry pickers reflects the impact of building 4 bays at once to shorten the overall assembly time. The 7.5 m beam builder which fabricates the interface tribeam supports is also included. However, available study resources precluded equivalent analysis to define the full array of equipment needed to assemble the laser power transmission system and the elements of the interface system. As previously discussed, many diverse construction operations must be performed to assemble all of the elements in these systems. Although a breakdown of the power transmission/interface assembly equipment remains to be developed, it is believed that the total mass and cost of these items will be similar to those for building the concentrator.

A comparison of crew operations staffing for the reference GEO base and for the laser construction base is shown in Figure 5-22. Each base operates on two 10 hour shifts per day and has similar organizations. Construction of the solar concentrator requires nearly three times as many people as does assembly of the reference energy conversion system because it has a denser structure and requires more construction equipment. The diverse construction operations for assembling the transmission system, however, have not been analyzed to the point where the sequence of operations and required equipments are defined. At this juncture it is believed that the crew size needed to assemble the transmission system will lie somewhere between 50% and 100% of the total crew used for solar concentrator assembly. The remaining construction operations (i.e., subassembly factory, maintenance, logistics and test/QC) are assumed to be the same for both concepts. In addition, the base operations and base management crew operations are also the same. However, the larger construction crew for the laser SPS leads to more people for base support (i.e., utilities, hotel, food service, etc).

### 5.2.4 Net Impact of IOP Laser SPS on GEO Base

Impact of IOP Laser SPS construction is summarized in Figure 5-23, in terms of penalty (or gain) to the reference GEO base mass, cost, and productivity. The

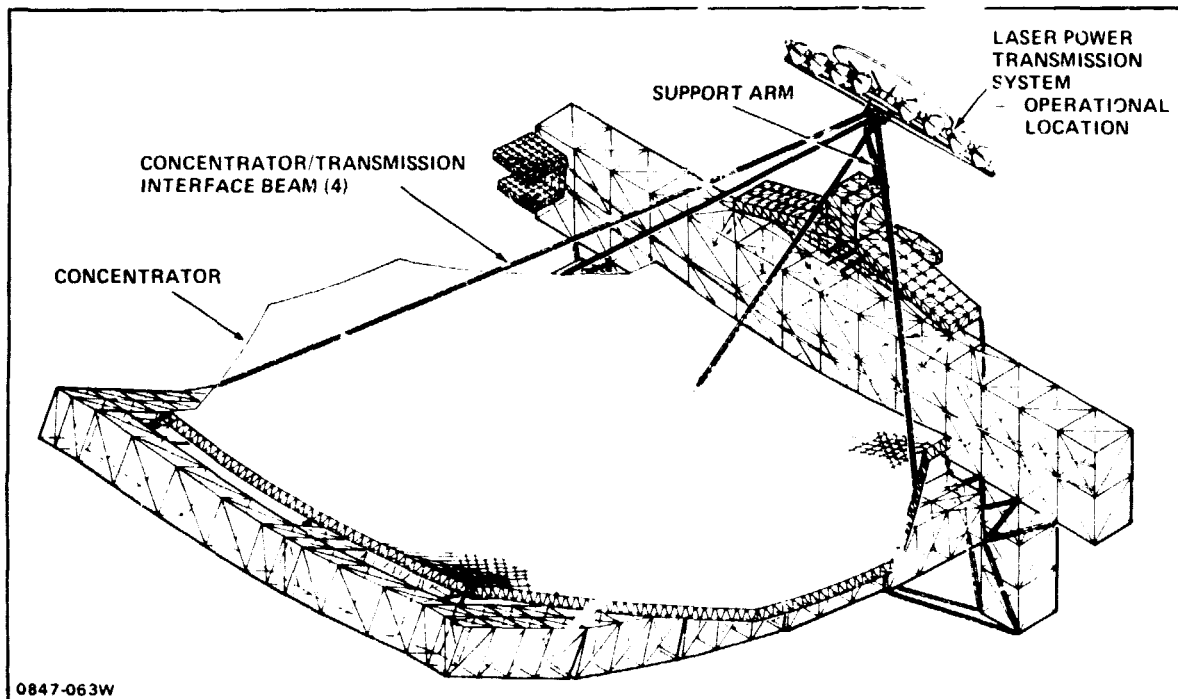


Figure 5-20 Laser SPS – Final Systems Mating

REF BASE  
DELTA  
• -26 MT  
• +\$1580M

CONSTRUCTION AREA/EQUIPMENT	QTY	MASS, MT	COST, SM
• CONCENTRATOR ASSEMBLY			
- BEAM BUILDERS			
1.5 m GIMBAL MANNED	18	72	724
1.5 m MOBILE MANNED	2	8	79
7.5 m MOBILE MANNED	1	11	58
- CHERRY PICKERS			
30 m	29	72.5	621
45 m	6	18	128
- INDEXERS			
10 m	8	8.7	26
45 m } SINGLE SUPPORT	6	7.8	21
60 m MULTI-SUPPORT	2	16	14
- FACET ASSEMBLY STATION	1	3	21
SUBTOTAL		217 MT	\$1692M
• PWR TRANSMISSION/INTERFACE ASSY			
- UNDEFINED EQUIPMENT FACTOR (100%)	TBD	217	1692
TOTAL		434 MT	\$3384M

Figure 5-21 IOP Laser SPS Construction Equipment

reference base is not suitable for building this small Laser SPS concept. An entirely different and much smaller construction base is needed. However, there are many diverse laser satellite assembly tasks to be performed on this smaller base, which leads to a larger crew size (587 vs 444). Hence, more habitats are required than for the reference 4 Bay End Builder. Although the total mass of the laser base is significantly less, the net effect increases the GEO base investment cost and annual operations cost as shown. For the IOP Laser Construction base defined, it was not practical to accelerate the concentrator assembly operation further to complete construction in less than 176 days. Consequently, productivity of the laser construction base is 2% of the reference. It is possible, however, that an alternate structural concept and another more highly automated construction facility could build the entire satellite a great deal faster.

CREW OPERATION	REFERENCE GEO BASE	LASER CONST BASE	
<b>CONSTRUCTION OPERATIONS</b>	<b>258</b>	<b>377</b>	
- ENERGY CONVERSION SYS	42	-	
- SOLAR CONCENTRATOR SYS	-	116	
- AP TENNA	42	-	
- POWER TRANSMITTER	-	87	
- SUBASSEMBLY FACTORY	48	48	
- MAINTENANCE	40	40	
- LOGISTICS	44	44	
- TEST/QC	42	42	
<b>BASE OPERATIONS</b>	<b>84</b>	<b>84</b>	
<b>BASE SUPPORT</b>	<b>84</b>	<b>108</b>	
<b>BASE MANAGEMENT</b>	<b>18</b>	<b>18</b>	
<b>TOTAL CREW</b>	<b>444</b>	<b>587</b>	
<b>Δ CREW</b>	<b>-</b>	<b>143</b>	

0847-065W

Figure 5-22 IOP Laser Constuction Base Crew Comparison

BASE PRODUCTIVITY  
IOP LASER SPS - 0.2 GW YR  
REFERENCE SPS - 10 GW YR

GEO BASE ELEMENT	Δ MASS, MT	COST - 1979 \$M	
		DDT&E	UNIT COST
• WORK FACILITIES			
- STRUCTURE	-2167	-34	-250
- CONSTRUCTION EQUIPMENT	- 26	0	1580
• CREW SUPPORT FACILITIES			
- 2.17 m DIA HABITATS	486		770
• WORKAROUND FACTORS			
- DEVMT 127%		-43	
- PROD. 47%			987
<b>TOTAL</b>	<b>-1707 MT</b>	<b>-577M</b>	<b>\$3087M</b>
			<b>\$3010M</b>
<b>ANNUAL OPERATIONS INCREASE:</b>			
SALARIES & TRAINING (+143)			212
RESUPPLY	+363 MT YR		204
			<b>\$416M YR</b>

0847-065W

Figure 5-23 IOP Laser SPS Construction Base Impacts

ORIGINAL PAGE IS  
OF POOR QUALITY





D180-25969-3

## **6.0 OPERATIONAL ASPECTS**

Pertinent aspects of a 30 year 10 Gw/year are tabulated on Tables 6-1 through 6-6. Except for satellite size, the FEL and EDL are comparable. However, the mixing gas IOPL generally has vastly greater requirements due to its increased complexity and 100 Mw instead of 1 Gw unit size.



D180-25969-3

Table 6-1 Laser SPS Operational Factors

OPERATIONAL FACTOR	LASER SATELLITE CONCEPTS			LASER RECTENNA CONCEPTS	
	MIXING GAS	FEL	EDL	PHOTOVOLTAIC	POWER TOWER
<b>INDUSTRIAL COMPLEX/SURFACE TRANSPORTATION</b> . Primary Industrial Capacity Needs . Surface Transportation	. Krypton . Graphite Fibers . Laser Optics	. Solar Array . Graphite Fibers . Klystrons . Laser Optics	. Solar Array . Graphite Fibers . Laser Optics	. Solar Array . Fresnel Lens or Optical Diodes	
	(ADDITIONAL MASS OF MATERIALS TO BE TRANSPORTED WILL NOT STRAIN THE CURRENT TRANSPORTATION SYSTEM)				
<b>RECTENNA CONSTRUCTION</b> . No. of 1 GW sites . Size of Sites				300 (1 x 1 km?) 320 x 320 m + Radiators + Switchyard + Exclusion Boundary	300 (1 x 1 km?) 320 x 320 m + Radiators + Switchyard + Exclusion Boundary
. No. of Sites to Bring On Line Each Year				10	10

Table 6-2 Laser SPS Operational Factors

OPERATIONAL FACTOR	LASER SATELLITE CONCEPTS			LASER RECTENNA CONCEPTS	
	MIXING GAS	FEL	EDL	PHOTOVOLTAIC	POWER TOWER
<b>RECTENNA CONSTRUCTION - Cont.</b> . Construction Complexity Factors				. Lens and support structure could be automated. . May need superconductors.	. Need portable heliostat assy. factory. . Power tower does not lend itself to high-rate construction
<b>LAUNCH AND RECOVERY SITE</b> . <u>Mass Laser SPS</u> . Microwave-to-Ref. Mass Ratio . No. of 400 MT HLLV's in fleet . No. of Launches per Week . No. of Launch Pads . Location of Launch Site	6 36 48 18	2.25 14 18 7	6.4 38 51 19		
	(NONE OF THESE COULD BE SUPPORTED BY KSC-- WOULD HAVE TO GO TO OFFSHORE OR EQUATORIAL SITES)				

ORIGINAL PAGE IS  
OF POOR QUALITY

**Table 6-3 Laser SPS Operational Factors**

OPERATIONAL FACTOR	LASER SATELLITE CONCEPTS			LASER RECTENNA CONCEPTS	
	MIXING GAS	FEL	EDL	PHOTOVOLTAIC	POWER TOWER
1. LEO BASE					
• EOTV Fleet Size	132	50	141		
• Time required to construct EOTV fleet at 8 vehicles/year rate	16.5 yrs	6.25 yrs	17.6 yrs		
• No. of LEO Bases required to construct EOTV fleet within 9 years (vehicle life)	2	1	2		
• No. of HLLV docking ports	18 (9 on each base)	7	19 (10 on each base)		
	(HAVING HLLV DOCKING PORTS ON MULTIPLE SIDES OF THE BASE WILL PRESENT APPROACH/DEPARTURE OPERATIONAL PROBLEMS)				
• No. of EOTV's in stationkeeping positions	6 (could pose an operational problem)	2-3	6-7 (could pose an operational problem)		

**Table 6-4 Laser SPS Operational Factors**

OPERATIONAL FACTOR	LASER SATELLITE CONCEPTS			LASER RECTENNA CONCEPTS	
	MIXING GAS	FEL	EDL	PHOTOVOLTATIC	POWER TOWER
C. SPACE TRANSPORTATION					
No. of EOTV's in pipeline	132	50	141		
No. of POTV's in pipeline	120	4	8		
No. of Cargo Tugs	12 @ LED 12 @ GEO	6 @ LED 6 @ GEO	12 @ LED 12 @ GEO		
D. GEO BASE					
No. of Construction Bases Req'd to Bring 10 GW Capacity On-Line <sup>a</sup> ch yr	50	2	2		
Construction Crew Size at Each Base	587	450	900		
Total Number of Construction Crew	29,350	900	1,800		

<sup>a</sup> Penalty is small compared to Mixing Gas IOPL

\* Penalty is small compared to Mixing Gas IOPL

ORIGINAL PAGE IS  
OF TYPE QUALITY

**Table 6-5 Laser SPS Operational Factors**

OPERATIONAL FACTOR	LASER SATELLITE CONCEPTS			LASER RECTENNA CONCEPTS	
	MIXING GAS	FEL	EDL	PHOTOVOLTATIC	POWER TOWER
UTILITY GRID					
. Input to Grids in "Small" Increments				100 MW - 1 GW	100 MW - 1 GW
. Intermittent Input Due to Weather					
. (Other Power Input Interruptions Essentially The Same as for Microwave SPS)					
. Rectennas will be Predominantly Located in Arid Locations					
. Smaller Unit Size Allows Rectennas to be Located Near to Population Centers					
. Tolerance to Winds, Earthquakes, Ice, Snow, etc.				Fresnel Lens will be susceptible to damage	Should be easier to protect heliostats from damage.

**Table 6-6 Laser SPS Operational Factors**

OPERATIONAL FACTOR	LASER SATELLITE CONCEPTS			LASER RECTENNA CONCEPTS	
	MIXING GAS	FEL	EDL	PHOTOVOLTAIC	POWER TOWER
a. COMMAND CONTROL  Increased Number of Space Vehicles and Bases will Demand Much More Complex C&C System. (Space Traffic Control, Tracking and Comm, Base Support C&C, etc.)  Will Require N times the Number of Orbital Slots	100	10	10		

**D180-25969-3**

## **7.0 NEW TECHNOLOGY**

**No new technology was developed as a result of this study.**

## **8.0 CONCLUSIONS**

The most promising laser for the SPS application is the free electron laser. The various laser option masses are compared on Figure 8-1. The FEL is inherently lighter, scales nicely to commercial utility power levels, and exhibits a distinct advantage in having a tunable wavelength to enhance atmospheric transmission. While the IOPL is the next lightest option, it also has great room for improvement via better laser catalysts, lighter radiators, and lighter gas separation systems.

Since almost all aspects of laser SPS's require technology which is not common practice today, it might be argued that an immense amount of new technology is required. Compared with the microwave reference SPS this is undoubtedly true. On the other hand, almost all of the technical aspects of the concepts proposed here appear readily possible if approached correctly - we know of no "can't possibly do" in the results presented in this report.

ORIGINAL PAGE IS  
OF POOR QUALITY

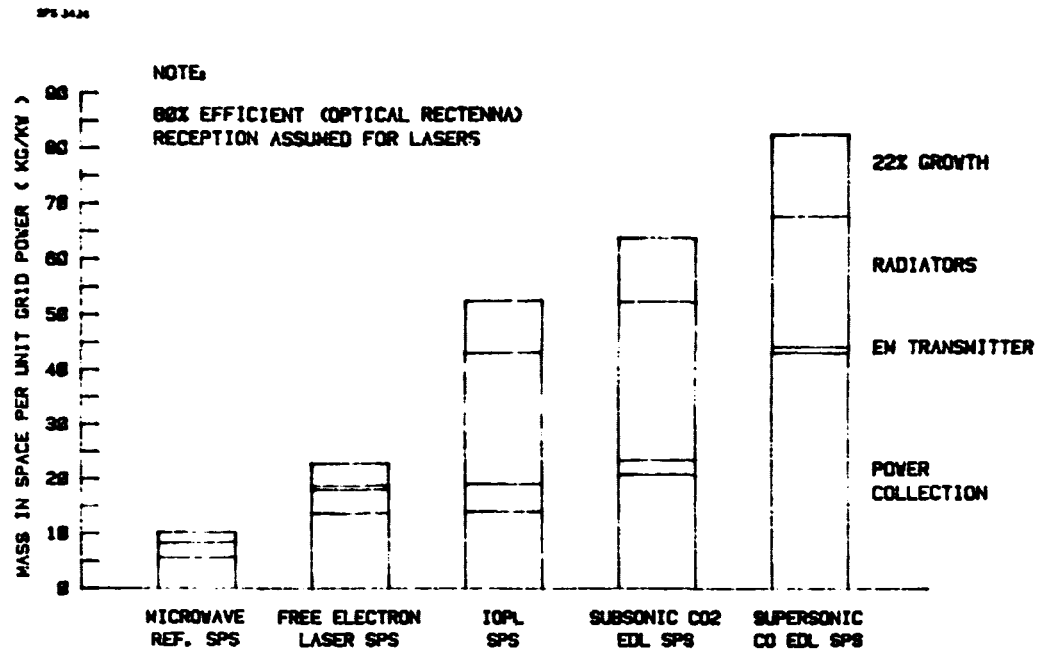


Figure 8-1: Laser SPS Option Masses Compared

## 9.0 RECOMMENDATIONS

In order to gain early information as to the technological feasibility of the laser alternative for the SPS, these recommendations are aimed at the first three years of the SPS Ground Based Exploratory Development (GBED) program. Additional activities which can be considered on an optional basis and at lower priority include the development of a low mass supersonic CO electric discharge laser optimized for atmospheric transmission and a search for better lasants and lighter solar collectors for use with direct solar pumped lasers. Neither of these laser types should be absolutely excluded from consideration in the GBED even though they are presently not the best candidates.

Considering both the promise and the relative immaturity of these laser technologies, we recommend the following items for further research:

### ELECTRON DISCHARGE LASERS

1. Investigate any potential concepts that might a) improve EDL efficiencies or b) raise their heat rejection temperatures.
2. Investigate laser window materials.
3. Perform more extensive analysis of EDL laser module scale-up effects on system control and performance.

### INDIRECT OPTICALLY PUMPED LASER

1. Investigate promising laser catalysts to improve selective depopulation of the CO<sub>2</sub> ground state during lasing.
2. Develop better alternates to conventional cryogenic techniques for separating the CO<sub>2</sub> and catalysts from the CO.
3. Analyze techniques for radiation at higher temperatures in the laser gas loop and/or lighter weight radiator concepts.

#### D180-25969-3

4. Carry out systems analysis to correctly scale IOPL lasers or amplifiers to allow a workable control system and to minimize mass in orbit per unit busbar power on the ground.
5. Conduct a proof-of-concept experiment to verify the performance of the most promising IOPL laser. (There is currently no ongoing work on this topic and none is planned by other organizations.)

#### FREE ELECTRON LASER

1. Examine detailed constraints on higher power operation (i.e., 10 MW to 1 GW) of electron beams, accelerators and FEL wiggler.
2. Investigate glancing optics to reduce intercavity distances.
3. Determine optimal transmission wavelength(s) in terms of mass in orbit per unit power delivered in electricity on the ground.
4. Analyze results of ongoing FEL proof-of-concept experiments. (These are currently under way with sponsorship from DARPA and other organizations.)
5. Evaluate the desirability of conducting similar experiments (at the MSNW/Boeing facility or elsewhere) to verify performance at FEL wavelength desired for SPS applications.

#### ALL LASERS

1. A reliable optical beam control system is a must for these systems to be feasible, yet it has to be proposed or developed in a comprehensive fashion. Because this is probably the most essential technology it should receive highest priority in a laser SPS program.



## LASER POWER RECEIVERS

1. Laboratory proof of concept experiments can and should be easily done for all the proposed power receiver concepts.
2. Propagation effects need to be analyzed and experimentally investigated as part of a continuing program. (An existing laser propagation research program might be given this mandate if it is applicable.)

END  
DATE  
FLMED  
9-8-80